



HAL
open science

The syn-rift tectono-stratigraphic record of rifted margins (Part I): Insights from the Alpine Tethys

Gianreto Manatschal, Pauline Chenin, Jean-françois F Ghienne, Charlotte Ribes, Emmanuel Masini

► **To cite this version:**

Gianreto Manatschal, Pauline Chenin, Jean-françois F Ghienne, Charlotte Ribes, Emmanuel Masini. The syn-rift tectono-stratigraphic record of rifted margins (Part I): Insights from the Alpine Tethys Basin Research, inPress, 10.1111/bre.12627 . insu-03473211

HAL Id: insu-03473211

<https://insu.hal.science/insu-03473211v1>

Submitted on 9 Dec 2021

HAL is a multi-disciplinary open access archive for the deposit and dissemination of scientific research documents, whether they are published or not. The documents may come from teaching and research institutions in France or abroad, or from public or private research centers.

L'archive ouverte pluridisciplinaire **HAL**, est destinée au dépôt et à la diffusion de documents scientifiques de niveau recherche, publiés ou non, émanant des établissements d'enseignement et de recherche français ou étrangers, des laboratoires publics ou privés.

1 **THE SYN-RIFT TECTONO-STRATIGRAPHIC RECORD OF**
2 **RIFTED MARGINS (PART 1): INSIGHTS FROM THE**
3 **ALPINE TETHYS**

4
5 G. Manatschal¹, P. Chenin¹, J.F. Ghienne¹, C. Ribes² and E. Masini³

6 *1* Institut Terre et Environnement de Strasbourg, UMR 7063, Université de Strasbourg, CNRS, 5
7 rue Descartes, Strasbourg F-67084, France

8 *2* Total, Pau, France

9 *3* M&U SAS, Saint-Egreve, France

10

11 **ABSTRACT**

12 The tectono-stratigraphic evolution of rift systems is at present poorly understood, especially
13 the one preceding the onset of oceanic seafloor spreading. Improving our understanding of the
14 complex, polyphase tectonic evolution of the fossil Alpine Tethys, one of the best calibrated
15 magma-poor rift systems worldwide, offers great potential for the interpretation of the distal
16 part of global rifted margins, which notoriously lack data. In this paper, we propose a tectono-
17 stratigraphic model for the former Alpine Tethys, whose remnants are exposed in the Alps of
18 Western Europe. We first review the historical evolution of some concepts grounding present
19 knowledge on the Alpine- and global magma-poor rifted margins. Then we present a spatial
20 and temporal template for the Alpine Tethys rift system using a “building block (BB)”
21 approach. This new approach is powerful in that it can integrate high-resolution, structural,
22 stratigraphic, thermochronological and petrological observations from dismembered outcrops
23 into a margin-scale template compatible with the first-order seismic architecture defined at
24 present-day, magma-poor rifted margins. The detailed analysis of the syn-rift sequence of the
25 Alpine Tethys margins demonstrates that extension migrated and localized while evolving from
26 the stretching to the necking phase. During hyperextension, rifting was asymmetric and
27 controlled by in-sequence detachment faulting. Then, the rift system evolved back into a more
28 symmetric, embryonic spreading system. With this contribution, we aim to allow readers
29 without knowledge of the Alps to access to this unique “archive” preserving some of the world’s
30 best-exposed rift structures. Recognising these structures is critical to understand the origin of
31 some new concepts used to explain present-day, deep-water rifted margins, and to interpret and
32 predict the tectono-stratigraphic evolution during advanced stages of rifting.

33

34 **Highlights:**

35 Our “building block” approach enables us to upscale local outcrop observations into a global
36 margin template

37 The syn-rift sequence of the Alpine Tethys margins is among the best calibrated worldwide

38 The observed rift migration - localization has far-reaching consequences for the interpretation
39 of global rifted margins

40

41 **Keywords:** Alps, Alpine Tethys, tectono-stratigraphic evolution, polyphase rifting

42 INTRODUCTION

43 **Why revisit the syn-rift sequence of the Alpine Tethys?**

44 In the past two decades, our understanding of the architecture and evolution of rifted margins
45 in general, and of the distal parts of magma-poor rifted margins in particular, have been greatly
46 enhanced (Péron-Pinvidic and Manatschal, 2019). Field studies in the Alpine Tethys have
47 played a key role in the development of new concepts. Indeed, there are few places where the
48 syn-rift sequence of a conjugate, magma-poor rifted margin is so well exposed, including the
49 most distal parts, and where rift-related structures have been examined in such detail. These
50 studies, closely linked to the progress in seismic imaging and modelling of rifted margins, have
51 enabled development and testing of many new concepts of rifted margin formation. They also
52 helped understanding the latest stages of the rifting process (i.e., the breakup phase), the related
53 tectono-stratigraphic evolution, as well as the resource potential in poorly calibrated distal
54 margins. The spatial and temporal characterization of rifted margins is a prerequisite to generate
55 better plate tectonic/geodynamic reconstructions, and to understand the formation of a plate
56 boundary, a first-order plate tectonic process that remains yet little understood.

57 This paper focuses on the rift-related stratigraphy and tectonic evolution of the Jurassic Alpine
58 Tethys rift system. Here we use the term “Alpine Tethys” to refer to the (proto-)oceanic
59 domain(s) and related conjugate rifted margins separating the European-Iberian and African-
60 Adriatic (micro)continents (Fig. 1a). We use the term rifting to refer to the process thinning the
61 crust from its initial thickness (30 ± 5 km) to less than 30 km. We present an historical overview
62 of the key observations and data that are at the origin of some recent concepts on rifted margin
63 formation based on more than one century of research in one of the world’s best investigated
64 orogens. As this review can obviously not include all details and refer to all studies published
65 over more than a century, we focus on the more recent discoveries, in particular on the distal
66 parts of the Alpine Tethys margins.

67 **Geological and paleo-geographical setting**

68 From a broad-scale perspective, the Alpine Tethys formed contemporaneously with the
69 subduction of the Paleo- and/or Neo-Tethys Ocean(s) to the east, and with the opening of the
70 Central Atlantic to the west (Fig. 1b). Aside from the Alpine Tethys, other extensional basins
71 such as the *Meliata-Vardar* and the *Pyrenean-Bay of Biscay* (Fig. 1a) formed between the
72 Paleo- and/or Neo-Tethys and Atlantic domains, from the Late Triassic to Cretaceous (Handy
73 et al., 2010). These (proto-) oceanic domains developed successively westwards, resulting in a
74 complex, so-called *multi-stage*, plate-kinematic framework that will be discussed later.

75 The Alpine Tethys evolution is part of a *Wilson Cycle* that may have been incomplete, in the
76 sense that neither seafloor spreading, nor subduction reached a steady-state evolution (Chenin
77 et al., 2018a). It initiated at the end of the late- to post-orogenic collapse of the Variscan Orogen,
78 which led to peneplanation in Western Europe, as recorded in the widespread Late
79 Carboniferous to Permian depocenters. The stratigraphic development of these depocenters and
80 their link to the Permian and Triassic volcanics and thick Triassic platforms observed in the

81 Adriatic and Briançonnais domains are ill constrained. At a super-regional scale, the Alpine
82 Tethys rifting initiated in the Late Permo-Triassic in the Dinarides, Hellenides, Turkey, Iran
83 and Oman (e.g., Stampfli, 1990 ; Robertson & Searle, 1990). In the Vardar in Greece, rifted
84 margins and fringing MORB crust is dated following the Permo-Triassic rift phase (van
85 Hinsbergen et al., 2020). Rifting localized in the Alpine Tethys during the so-called *necking*
86 *phase* in the late Sinemurian/Pliensbachian (185 ± 5 Ma) (Mohn et al., 2010). This phase
87 corresponded to both major crustal thinning and the formation of a segmented rift system
88 comprising three basins, namely from southwest to northeast, the Ligurian, Piemonte and Valais
89 basins (Fig. 1a). These basins merged in a continuous, proto-oceanic domain, linking the
90 Central Atlantic with the Tethys realm (Baumgartner, 2013) during the subsequent phase of
91 mantle exhumation. Mantle exhumation initiated during the Callovian/Bathonian (165 ± 5 Ma)
92 (Ribes et al., 2019) and was associated with incipient magmatic activity. Whether the Alpine
93 Tethys eventually developed into a mature, steady-state spreading system remains debated. At
94 present, observations and data do not support the existence of a mature Penrose crust in the
95 Alpine Tethys domain, but that it existed cannot be excluded. The nature and width of the
96 Alpine Tethys oceanic or proto-oceanic domain have direct implications on a second debate
97 related to the nature of the subsequent Late Cretaceous to early Cenozoic Alpine subduction.
98 While McCarthy et al. (2020) suggested that the Alpine Tethys was closed via an Ampferer-
99 type subduction (i.e., closure of narrow hyperextended rift basins with immature subduction
100 zones and without formation of Arc magmatic activity), Handy et al. (2010) proposed a more
101 classical model involving subduction of a wider and mature oceanic domain. Whatever the
102 nature of the oceanic domain(s) and subduction in the Alps, the fact is that there is little evidence
103 for a mature oceanic domain and Pacific-type subduction. Indeed, most of the rocks exposed in
104 the Alps are derived from the former Tethyan margins (Fig. 1c).

105 At present, remnants of the Alpine Tethys margins are scattered along the Alpine belt, over an
106 area that extends from the Carpathians to the Apennines and further southwest in the Tell, Betics
107 and Rif regions of northern Africa. In this paper we focus on examples that are assigned to the
108 Adriatic margin and exposed in the Austroalpine and south Penninic nappes of southeastern
109 Switzerland and northern Italy; and on the other hand, on the former European margin exposed
110 in the Western and Central Alps of W-Switzerland, SE France and NW Italy (Figs. 1c and 1d).
111 The northeastern and southwestern terminations of the Alpine Tethys (Fig. 1a) are less well
112 understood due either to a more complex rift evolution or a stronger overprint by the later,
113 subduction-related, back-arc extension (Pannonian Basin, Gulf of Lyon and Tyrrhenian Sea;
114 Schettino and Turco, 2011). The link between the rift structures and the later Alpine
115 reactivation, as well as how remnants of the former rifted margin were emplaced and partly
116 preserved in the Alpine nappe stack is not directly addressed in this study, and we refer to the
117 studies by Mohn et al. (2011); Beltrando et al. (2014) and Epin et al. (2017) for further
118 discussion. A review discussing the role of rift inheritance in building collisional orogens can
119 be found in Manatschal et al. (2021).

120

121 A major, so far unresolved problem in describing the Alpine Tethys is linked to the difficulty
122 in proposing robust paleogeographic and kinematic reconstructions. The main problem arises
123 from the kinematics of the Iberia plate (Vissers & Meijer, 2012; Barnett-Moore et al., 2016;
124 Nirrengarten et al., 2018) because different positions of the Iberia plate imply different widths
125 of the Alpine Tethys. First, whether the magnetic anomaly M0/J in the southern North Atlantic

126 represents an oceanic magnetic anomaly is debated. If it is not, it cannot be used for restorations.
127 Second, most of the rifting west and north of Iberia occurred during the Cretaceous magnetic
128 superchron and is, therefore, not recorded in the magnetic tape recorder. More recent studies
129 (Nirrengarten et al., 2017; Szameitat et al., 2020) showed that the M0/J anomalies in the
130 southern North Atlantic did not form on “true” oceanic crust, and can therefore not be used for
131 kinematic restorations. As a consequence, older restorations for the Alpine Tethys relying on
132 the M0/J magnetic anomaly as an isochron (e.g., Handy et al., 2010; Vissers et al., 2012; Van
133 Hinsbergen et al., 2014) must be taken with care. Here we use the interpretation of Decarlis et
134 al. (2018), who suggested a segmentation of the Alpine Tethys into two sub-basins (Ligurian
135 and a Piemonte), separated by a Jurassic transform system, like Handy et al. (2010) (Fig. 1a).
136 Based on this assumption, the Grischun transect discussed in this paper (B''–B''') section in
137 Figs. 1a and 1c) was part of the Piemonte segment of the Alpine Tethys and was conjugate to
138 the southeast European margin currently exposed in Sardinia and Calabria (Costamagna, 2016).
139 Although this hypothesis needs to be further confirmed, we note that it is consistent with
140 reconstructions by Angrand et al. (2020) and Le Breton et al. (2020).

141 **Historical overview**

142 As pointed out by Şengör (2014), the Alps of Western Europe are likely the place where most
143 new concepts on the formation of rift and oceanic domains and their emplacement in orogens
144 have been developed (Fig. 2). Major steps in the evolution of the Alpine Tethys and the
145 characterisation of paleogeographic domains were the pioneering works of Suess (1883; Fig.
146 2a), Steinmann (1905; Fig. 2b) and Argand (1916; Fig. 2c). Concerning the compressional
147 reactivation, Bertrand (1884) and Haug (1892) were among the first to demonstrate the evidence
148 of “nappes” in the Alps. Haug (1892) associated the emplacement of the nappes with the
149 deposition of the Oligocene Flysch deposits. Termier (1899) then demonstrated that the Alps
150 were formed by a stack of different “nappes”. Haug (1909) and then Argand (1916) defined a
151 succession of pre-nappe geosynclines and geanticlines in the Alps, which were the precursors
152 of what we now refer to as rift basins and rifted margins. Haug (1909) also described the
153 occurrence of breccias on the flank of the geanticlines, which he interpreted to result from
154 submarine slumps that were interbedded with deeper marine sediments of the two neighbouring
155 geosynclines.

156 The start of a more modern view of rifted margins was initiated in the 1960's with the studies
157 of Elter and Lemoine (Figs. 2d and 2e). Lemoine (1961, 1967) reconsidered the ideas proposed
158 by Haug (1909), and showed that the structure and related stratigraphy observed in the Alps
159 resulted from Jurassic and Cretaceous extension. In the same period, Bernoulli (1964) mapped
160 the first fault-bounded rift basin in the southern Alps (the Generoso Basin). Field observations
161 from the Alpine Tethys were compared with the first DSDP drilling results in the Central
162 Atlantic, other present-day rift basins, and seismic images of the Bay of Biscay (Montadert et
163 al., 1979; Weissert & Bernoulli, 1985). With the advent and success of *Plate Tectonics*, it was
164 generally accepted in the early 1980's that the Alpine Tethys was floored by “Penrose-type”
165 oceanic crust and was flanked on both margins by latest Triassic to Late Sinemurian, fault-
166 bounded rift basins (Lemoine et al., 1987; Eberli, 1988, Bertotti et al., 1993). As a consequence,
167 stratigraphic contacts between mantle and sediments or between mid-crustal rocks and
168 sediments, nicely described as “pre-Alpine” prior to Plate Tectonics (e.g., Steinmann, 1905;

169 Decandia & Elter, 1969; Dietrich, 1970; Trümpy, 1975), were reinterpreted as being Alpine
170 (Hsü & Briegel, 1991). The fact that the ophiolites looked peculiar and did not fit into the classic
171 three-layered, Penrose-type oceanic crust led the community to assume that they were heavily
172 overprinted, destroyed or subducted during Alpine convergence.

173

174 It was only in the late 80's and early 90's, when serpentized mantle rocks were drilled
175 offshore Iberia (Boillot et al., 1987), and detachment systems were described in the
176 Southwestern United States (Wernicke, 1985), that geologists started to reconsider previously
177 reported field observations of exhumed mantle (Decandia & Elter, 1969, 1972; Florineth &
178 Froitzheim, 1994; Lagabrielle, 1994) and detachment faults (Froitzheim & Eberli, 1990;
179 Froitzheim & Manatschal, 1996). These concepts were reintroduced in the interpretations of
180 the Alpine Tethys (Lemoine et al., 1987; Froitzheim & Eberli, 1990; Lagabrielle & Cannat,
181 1990) and applied to present-day "magma-poor" rifted margins (Whitmarsh et al., 2001).

182

183 The significant progress in understanding rifted margins accomplished during the last decades
184 (e.g., 1990-2020) is intimately linked to the development of new, high-resolution seismic
185 imaging methods and numerical modelling (Péron-Pinvidic and Manatschal, 2019). However,
186 access to and comparison with field analogues (Whitmarsh et al., 2001; Lavier & Manatschal,
187 2006) were fundamental in establishing new concepts for rifted margins. Seismic imaging of
188 entire rifted margins and attempts to model the way they form provided a first-order
189 understanding of rift evolution. However, without drillhole data from deep-water rifted
190 margins, which enabled us to compare the nature of contacts (unconformities or faults) as well
191 as document ages and depositional settings of sediments, it would not have been possible to
192 identify the processes occurring during the final stage of rifting, immediately prior to
193 lithospheric breakup and seafloor spreading. Conversely, it would not have been feasible to
194 establish new concepts on the tectono-stratigraphic understanding of rifting based on the
195 fragmented observations derived from the Alps only. Thus, it was historically (and it is still)
196 the combination of onshore and offshore geological studies that enabled development and
197 constraints to be placed on new concepts for the processes occurring at higher β -factors when
198 extending the crust and/or lithosphere.

199 **FROM DISPERSED OUTCROPS TO THE ARCHITECTURE OF THE** 200 **ALPINE TETHYS**

201 The Alpine Tethys margins have been partly accreted and subducted during the multi-stage
202 Cretaceous and Tertiary Alpine compressional events. Thus, when referring to Tethyan margins
203 in the Alps, we actually mean "remnants" of the former margins, now embedded in the Alpine
204 nappe stack. Restoring the former margins of the Alpine Tethys relies on the one hand on the
205 recognition of its remnants, and on the other on our ability to relocate them within the pre-
206 Alpine rift template. Such a reconstruction is neither easy, nor is there a unique solution.

207 In the following section, we explain how to build a template for the Alpine Tethys margins. In
208 particular, we describe: (1) the concept of "building blocks" (BB); (2) how to locate the BB in
209 the spatial Alpine Tethys margin framework; and (3) how reliable the proposed template is and

210 what data are missing to improve and better constrain the understanding of the Alpine Tethys
211 tectono-stratigraphic evolution. A major aim of this paper is to integrate the concepts and their
212 derived terminologies used to describe the Alpine Tethys margins into a coherent language
213 accessible to readers from different geological backgrounds, including those who are not
214 familiar with Alpine geology. In order not to overwhelm the reader with local details, names of
215 facies, structures or nappes that sometimes change across national or language borders, we
216 mention them as sparingly as possible and refer to the original papers where the reader can find
217 further details and explanations.

218 **Datasets and building blocks**

219 To restore the Alpine Tethys rifted margins, we define so-called “building blocks” (BB) (Fig.
220 3 and Tab. 1). BBs are ideally kilometre-scale outcrops, where primary rift relationships
221 between basement rocks, fault structures and syn-rift stratigraphic levels are preserved. BBs
222 provide therefore information about the: (1) nature of the basement (continental crust, exhumed
223 mantle or fully magmatic crust); (2) depositional environments and stratigraphic thickness, and
224 hence indications on accommodation, which can be used as a proxy for first-order crustal
225 thickness by applying isostatic principles (e.g., Tugend et al., 2014); and (3) geometry and age
226 of rift structures. In the Alps, seven types of BBs can be described. In the following, we refer
227 to them as BB1, BB2, ... BB7, and exemplify each one with one or several type-localities (Figs.
228 3a, 3d and 3e and Tab. 1).

229 BB1 (Fig. 3a and Tab. 1) displays classical tilted blocks and half graben bounded by high-angle,
230 normal faults. Normal faults affect a 30 ± 5 km thick crust, including possible pre-rift
231 sedimentary layers. The syn-tectonic deposits thicken and diverge towards the bounding faults,
232 and the corresponding depocenter can be several tens of kilometres in width and several
233 kilometres in depth (see dark blue layer in BB1; Fig. 3a). Crustal extension is typically low (β
234 < 1.5), and the total accommodation is minor, as indicated by the facies of the syn- and post-
235 rift sediments, in line with a bathymetry remaining shallow to moderately deep (< 500 m). The
236 type locality of BB1 is the Il Motto block in the Upper Austroalpine unit exposed near Livigno
237 in northern Italy (Eberli, 1988) (Figs. 4d and 4e). Other examples are the Generoso Basin in the
238 Southern Alps (Bernoulli, 1964) and the Bourg d’Oisans basins in the Western Alps (Lemoine
239 et al., 1986). BB1 is the most classical building block of rifted margins and failed rifts. It has
240 been extensively recognized and described from both intracontinental rifts and proximal rifted
241 margins since the 1960’s. (e.g., Gawthorpe & Leeder, 2000; Gupta et al., 1998).

242 BB2 (Fig. 3a and Tab. 1) shows crustal-scale shear zones typically juxtaposing upper and lower
243 crustal levels via the attenuation of ductile crustal layers, responsible for major crustal
244 thinning/necking. An example of BB2 is the Eita shear zone and Grosina detachment fault,
245 exposed in the Middle Austroalpine Grosina/Campo Nappe at the Swiss-Italian border (Mohn
246 et al., 2012; 2014) (Figs. 3d et 3e). The link between basement structures and the stratigraphic
247 record is, however, not well constrained in this area. More recent studies in the Mont Blanc
248 Massif (Western Alps; Ribes et al., 2020a) and in the Cusio-Biellese Zone (Southern Alps;
249 Beltrando et al., 2015; Decarlis et al., 2018) both considered as examples of BB2 ((Figs. 3d et
250 3e), enabled to investigate the surface expression and its link to the sedimentary evolution
251 during lithospheric/crustal necking. Both sites display evidence for mid-crustal basement
252 exhumation linked to detachment faults, erosion and deposition of basement-derived material
253 in shallow marine silicilastic sequences. The isostatic evolution recorded in the BB2 is complex

254 and suggests uplift, followed by rapid subsidence and sediment aggradation. The total
255 accommodation and tectono-sedimentary evolution related to BB2 are yet little investigated
256 and will be discussed in the accompanying paper (Chenin et al. same volume).

257 BB3 (Fig. 3a and Tab. 1) displays a major unconformity, also referred to as “the Briançonnais
258 unconformity”. This prominent syn-rift unconformity covers the tilted and eroded Triassic and
259 lower Jurassic platform carbonates and is draped by upper Middle to Upper Jurassic pelagic
260 carbonates. It is recognized throughout the Western and Central Alps in the so-called
261 Briançonnais nappes (Lory 1860; 1866; Kilian, 1891; Haug, 1909; Debelmas, 1955; and
262 Lemoine, 1961) and represents a major characteristic of the former distal European margin.
263 Crustal thickness of this block is difficult to determine, but by comparison with present
264 analogues, we reckon it to be 20 ± 5 km. BB3 is typically affected by high-angle faults with
265 minor offset. The type locality of BB3 is the Fond Froid – Lac de l’Ascension area in the
266 Briançonnais nappes (Figs. 4d and e), near the city of Briançon (southeastern France; Claudel
267 and Dumont, 1999).

268 BB4 (Fig. 3a and Tab. 1) comprises successive, in-sequence long-offset extensional detachment
269 faults responsible for exhumation of mainly upper crustal levels at the seafloor (for details see
270 Epin and Manatschal, 2018). The exhumed basement is locally overlain by allochthonous
271 fragments of upper crust and pre-rift and early syn-rift sediments. These structures are covered
272 by syn-tectonic and post-tectonic deep-water sediments (for details see BB4 in Fig. 3a). The
273 type-locality of BB4 is the Err-detachment system exposed in the Lower Austroalpine Err
274 Nappe north of the Julier Pass (Figs. 4d and e) (e.g., Froitzheim & Eberli, 1990; Manatschal &
275 Nievergelt, 1997; Masini et al., 2012; Epin & Manatschal, 2018). Another nearby example is
276 the Bernina detachment system (Mohn et al., 2012) (Figs. 4d and e).

277 BB5 (Fig. 3a and Tab. 1) is the least known block and, in contrast to the others, it is not
278 preserved in one single outcrop. A good description of the tectono-sedimentary relationships is
279 given in Ribes et al. (2019b). The main characteristic of BB5 is the occurrence of major breccia
280 bodies of Jurassic and/or Upper Cretaceous age that occur preferentially along the boundary
281 between the Briançonnais and the Piemonte units, or in units that are interpreted to derive from
282 the Valais basin (Fig. 4a). These breccias, first described by Haug (1909) and later by Lemoine
283 (1961; 1967), were interpreted as related to one or more submarine slopes that resulted from
284 either large faults or flexure. Ribes et al. (2019b) subsequently linked these breccias to
285 submarine mega-fault scarps that are more favourably formed along an upper plate setting
286 (Masini et al., 2013; Hauptert et al., 2016; Ribes et al. 2019b). Type localities of BB5 are the
287 Breccia Nappe in the Préalpes (Chessex, 1959; Badoux, 1962; Hendry, 1972; Weidman, 1972;
288 Escher et al., 1993; Steffen et al., 1993) (Figs. 4d and e). Other examples are the Monte Galero
289 breccia system (Decarlis et al., 2015) and the Falknis breccia (Ribes et al, 2020b).

290 BB6 (Fig. 3a and Tab. 1) displays tectonically exhumed serpentized mantle capped by
291 extensional detachment faults and ophicalcites, which are then overlain by deep-water, typically
292 silica-rich sediments. The nature of the mantle is subcontinental (Mantle-type 1 of Picazo et al.,
293 2016). The type locality is the Tasna ocean-continent transition (OCT) exposed north of Scuol
294 in the Lower Engadin valley (Florineth & Froitzheim, 1994; Manatschal et al., 2006; Ribes et
295 al. 2020b) (Figs. 4d and e). Other examples are the Upper Platta unit (Epin & Manatschal,
296 2018), Northern Lanzo (Kaczmarek & Müntener, 2008) or the External Ligurides (Marroni et
297 al., 2002).

298 BB7 (Fig. 3a and Tab. 1) shows magmatic additions that form simultaneous to mantle
299 exhumation along high- and low-angle faults (for detailed descriptions see Manatschal et al.,
300 2011; Epin et al., 2019; Coltat et al., 2020). The exhumed, subcontinental mantle mantle is
301 infiltrated, i.e., reacted with rift-related magma, but did not melt and is not genetically linked
302 with the overlying basalts (Mantle-type 2 of Picazo et al., 2016). The OCT-basalts are related
303 to incipient magma production (Amann et al., 2020). The first sediments overlying this domain
304 are either tectono-sedimentary breccias reworking exhumed mantle, or radiolarian cherts (Ribes
305 et al., 2019a). The type-locality is the Lower Platta Unit exposed in the Surses valley in
306 Grischun (Demurs et al., 2001) (Figs. 4d and e). Other examples are the Chenaillet Ophiolite
307 (Manatschal et al., 2011) (Figs. 4d and e), Southern Lanzo (Müntener & Piccardo, 2003) or the
308 Internal Ligurides (Tribuzio et al., 2004).

309 Not all observations derived from field studies in the Alps are considered in terms of BBs, and
310 yet they are important for the restoration of the former Alpine Tethys rifted margins. Examples
311 include the discovery of a fossil Moho in the Malenco unit (Hermann et al., 1997), and lower
312 crustal granulites linked to the intrusion of Permian gabbros in the Ivrea zone (Quick et al.,
313 1992; Barboza et al., 1999) and in the Sondalo region (Petri et al., 2016). These exposures
314 allowed us to understand the pre-rift crustal structure and inheritance as well as to better
315 understand the pre-rift lithospheric conditions, to determine the basins exhumation history, and
316 to assess the Pressure-Temperature-time (PTt) evolution of the basement rocks during rifting.

317 **Building a spatial template for Alpine Tethys rifted margins**

318 There are two ways to reconstruct a spatial template of the former Alpine Tethys margins. The
319 first one is to restore the Alpine nappe stack back to its initial pre-orogenic state. This approach
320 was first used by Argand (1916) (Fig. 2c), who was one of the first to consider a mobilistic view
321 and to describe a succession of adjacent paleogeographic domains each one with a characteristic
322 stratal record. More recently, Beltrando et al. (2014) and Epin et al. (2017) defined diagnostic
323 criteria to recognize remnants of the former rifted margins in the Alpine orogen and discussed
324 how they can be restored back to the pre-orogenic stage. However, these authors did not yet
325 develop the BB approach proposed here. A second way to restore fossil rifted margins is to
326 define a margin template based on isostatic considerations linked to geological observations
327 (nature of basement, top-basement, sediments as well as depositional environments and
328 sedimentary thickness; for a discussion of the approach see Tugend et al., 2014). This approach
329 resulted in the definition of rift domains. Linking this approach with the average width of
330 “modern” rift domains observed at present-day rifted margins (Chenin et al., 2017), and
331 assuming that the processes generating the margins are roughly similar, allows us to place all
332 the BBs of the Alpine Tethys conceptually along a modern margin template (red line profiles
333 in Fig. 3a). The BB approach presented in this study enables us to add to the definitions of
334 domains the key geological information that can be expected in each of the domains. By
335 combining all these approaches we can use the observations made in the Alps to establish a
336 more generic description of rifted margins and their evolution, a concept that will be used and
337 tested in the accompanying paper (part 2) of Chenin et al., in volume).

338 BB1, the “tilted blocks”, have been imaged since the 1970’s in the proximal margin (Montadert
339 et al., 1979). Until the late 1980’s, the entire margin was assumed to be formed by such
340 structures. Only with the discovery of exhumed mantle along the Iberia margin (Boillot et al.,

341 1987) made it clear that BB1 cannot explain the whole crustal structure of a magma-poor rifted
342 margin.

343 Lemoine et al. (1987) was the first to propose the existence of extensional detachment faults in
344 the Alps, but it was Froitzheim & Eberli (1990) who provided first field evidence for the
345 occurrence of such structures that characterize BB4. From the 1990's onwards, the structures
346 related to the former Adriatic margin in the Grischun transect (Figs. 1a and 3b) have been
347 decrypted. Eberli (1988) and Froitzheim & Eberli (1990) demonstrated that the proximal and
348 distal margins were controlled by different fault systems, namely pre-Sinemurian high-angle
349 faults in the proximal margin and post-Sinemurian detachment faults in the distal margin.

350 Lemoine et al. (1987) and Froitzheim & Manatschal (1996) proposed that the Alpine Tethys
351 margins had to be asymmetric based on the mapping of extensional detachment faults. Although
352 Decandia and Elter (1969) had already mentioned the existence of exhumed mantle, Florineth
353 and Froitzheim (1994) and Manatschal and Nievergelt (1997) presented field evidence for
354 extensional detachment faults related to mantle exhumation in the Tasna and Platta nappes,
355 which led to the definition of BB6 and BB7. Many studies had investigated the petrology of
356 magmatic and mantle rocks (Piccardo et al., 1990; Rampone et al., 1995, 1997; Müntener et al.,
357 2004), however the tectonic link between mantle exhumation along detachment faults and syn-
358 magmatic activity was only evidenced by Desmurs et al. (2001) and Epin et al. (2019) for the
359 Lower Platta unit (BB7), and by Manatschal and Müntener (2009) and Manatschal et al. (2011)
360 for the Chenaillet Ophiolite.

361 While the existence of exhumed mantle and related structures have been described and
362 generally accepted in the 1990's and early 2000's, the mechanisms of crustal thinning were, at
363 that stage, still poorly understood. The first models suggested that crustal thinning was
364 controlled by simple shear (Wernicke, 1985) and detachment systems (e.g., Lemoine et al.,
365 1987; Froitzheim & Manatschal, 1996). It was only Mohn et al. (2012) who identified evidence
366 for the necking process (BB2 fingerprints) based on field observations. Ribes et al. (2020) then
367 described the tectono-sedimentary evolution of this block, highlighting how and when the crust
368 underwent major crustal thinning.

369 Understanding and linking crustal thinning (BB2), mantle exhumation (BB6), and uplift and
370 subsidence of the future distal margin (BB3) during the evolution of the Alpine Tethys rifting
371 became possible thanks to the use of numerical modelling (Chenin et al., 2019, 2020). Finally,
372 to link massive breccia-bodies with rift models and define corresponding BB5, a detailed
373 tectono-stratigraphic investigation of the distal European margin was necessary (Ribes et al.,
374 2019b). Thus, it took more than 50 years to find and define the BBs, the combination of which
375 led to restore the first-order architecture of the Alpine Tethys margins.

376 Eventually, geologists identified and described BB's all over the Alps; however, it was only in
377 the Grischun transect (Figs. 1a and 3b) that the relative spatial template of the different blocks
378 could be directly restored by kinematic restoration of the Alpine nappe stack (Epin et al., 2017).
379 This exceptional preservation is due to the fact that all of the Adriatic margin remained in the
380 upper plate of the Alpine subduction and that it was most-likely located against a major pre-
381 Alpine transform system (the paleo-Subsibic line of the peri-Adriatic system; Fig. 4a)
382 (Manatschal & Nievergelt, 1997; Mohn et al., 2011; Epin et al. 2017). Indeed, in the Grischun
383 transect, five out of seven of the BBs have been identified in the nappe stack, each one in a
384 different nappe (Figs. 4d and e). The restoration of the nappe stack back to the pre-Alpine stage

385 (for details see Epin et al., 2017) enabled us to put the building blocks back to their relative
386 positions, with BB1 in the Ortler Nappe belonging to the proximal margin, BB2 in the Grosina-
387 Campo Nappe belonging to the necking zone, BB4 in the Err-Bernina Nappes belonging to the
388 hyperextended domain, and BB6 in the Upper Platta Unit and BB7 in the Lower Platta Unit
389 belonging respectively to the inner and outer part of the exhumed mantle domain (Fig. 3b). The
390 restoration of this nappe stack enabled us to assess the spatial distribution of these BBs across
391 the margin, but not to establish the detailed continuity and dimensions of the margin along
392 strike.

393 Concerning the European margin of the Alpine Tethys (Figs. 4d and e), BB1 occurs in the
394 proximal margin exposed in the Western Alps (Bourg d'Oisans). BB3, BB5 and BB6 in the
395 distal margin units exposed within the Penninic Nappes, and BB7 in the Chenaillet Ophiolite.
396 Remnants of BB5, the least understood BB, are preserved all along the Central and Western
397 Alps at the distal position of the Briançonnais domain and include the Falknis Breccia, the
398 Breccia Nappe, and the Monte Gallero Breccia (Decarlis et al., 2015; Ribes et al., 2019b). A
399 comprehensive restoration like that proposed for the Grischun transect is, however, not possible
400 for the European margin. The reason is that this margin has been more heavily affected by
401 multi-stage Alpine deformation. Indeed, most of the former distal parts of the European margin
402 were either subducted or destroyed during the Alpine collision. Moreover, the change in
403 kinematics from N-S to E-W-directed convergence renders the restoration of the nappe stack in
404 the Western Alps difficult (Rosenbaum et al., 2002).

405 **From 2D sections to a map view of the Alpine Tethys margins**

406 In order to reconstruct the three-dimensional architecture of the Alpine Tethys rift system, the
407 lateral continuity of the margins must be integrated. This requires us to first determine the extent
408 of distinct rift domains along dip (proximal, necking, hyperextended and exhumed
409 mantle/proto-oceanic domains (Fig. 3a)), and then to correlate and map them along strike. If
410 we assume that the width/scales of the Alpine margins are comparable to those of present-day
411 rifted margin domains (Chenin et al., 2017), we can also hypothesize paleogeographical maps
412 and sections of the former margins, and locate the BBs in such sections/maps in future studies.

413 A next step is to determine whether or not the rift system was segmented, and if so, to locate
414 the position of the main transfer zones. BB3 and BB5, which are characteristic of an upper plate
415 margin (hanging wall of the main extensional detachment system during hyperextension; e.g.,
416 Hauptert et al., 2016), are missing in the Grischun transect. This, together with the polarity of
417 exhumation faults (BB4; i.e., location of fault breakaways and transport direction), leave little
418 doubt that the distal part of the Grischun transect belongs to a lower plate margin (footwall of
419 the main extensional detachment system during hyperextension; Epin & Manatschal, 2018).
420 Based on an evaluation of the distribution of BB3, which is diagnostic for an upper plate margin,
421 Decarlis et al., (2018) proposed a change in the polarity from an upper- to a lower-plate margin
422 across a transfer fault that correspond to the Peri-Adriatic Insubric system. This observation
423 enabled us to define a pinpoint along the Adriatic margin, which can be linked to the
424 corresponding pinpoint on the conjugate European margin. Unfortunately, this pinpoint has not
425 yet been located on the European margin, which makes a restoration of the Alpine Tethys non-
426 unique for the time being. Our preferred view, which needs however to be confirmed by future
427 studies, is that the conjugate pinpoint lies at the southern limit of Sardinia and corresponds to
428 the paleo Iberia-European plate boundary. In such an assumption, the conjugate of the Grischun

429 lower plate transect would correspond to the Sardinia-Calabria section (Fig. 4). If correct, the
430 Sardinia-Calabria section would represent an upper-plate margin. Furthermore, following this
431 model, the Southern Alps and the Apennine (former Southern Adria margin), would correspond
432 to an upper plate margin and be conjugate to the Ebro/Balearian (lower plate) margin during
433 Jurassic rifting (Fig. 4a).

434 **THE SYN-RIFT TECTONO-STRATIGRAPHIC RECORD OF THE** 435 **ALPINE TETHYS**

436 With the BB approach explained in the previous chapter, it is possible to locate outcrops back
437 into the spatial template of the former Alpine Tethys margins. Some outcrops give access to
438 rocks derived from different pre-rift crustal and mantle levels, and thus provide information on
439 the thermal, spatial and isostatic evolution of the rift system. Such information is recorded by
440 the petrological, thermochronological and stratigraphic data., which enable us to: 1) define the
441 conditions and timing of crustal thinning, mantle exhumation and onset of magma production,
442 2) characterise the type of mantle and magma involved, and 3) describe the different spatial
443 isostatic/bathymetric evolution of rifting. In this section we describe how the tectono-
444 stratigraphic record of some of the key outcrops can help unravelling the chronostratigraphic,
445 structural and isostatic evolution of rifting.

446 **The stretching phase recorded in the proximal domains (BB1)**

447 The former proximal domains of the Alpine Tethys margins are preserved in the Dauphiné and
448 Helvetic nappes on the European margin, and in the Upper Austroalpine nappes and Southern
449 Alps on the Adriatic margin (Fig. 1). These domains are characterized by numerous half-graben
450 basins (Fig. 4c), some of the most emblematic are described below.

451 *The Bourg d'Oisans Basins (Figs. 4d, 4e and 5a)* located at the European margin include three
452 tilted blocks, namely from west to east the La Mure, the Taillefer and the Grandes Rousses.
453 These basement blocks are bounded by master faults, the best exposed and described being the
454 Ornon normal fault east of the Taillefer Block (Fig. 5a). The Ornon Fault had an approximate
455 throw of 1500 m (Barf ty, 1985) and largely controlled the formation of a c. 15 km-wide half-
456 graben. Chevalier et al. (2003) showed that diffuse extension initiated along numerous small
457 faults with limited throw and low strain-rate between the Hettangian and the Sinemurian, and
458 that these structures were widely distributed across the entire future proximal domain.
459 Extension then localized in Early Sinemurian, and most of the 1500 m throw was rapidly
460 accumulated along the single Ornon fault linked to a fast tectonic subsidence (Fig. 5a). Similar
461 to the other neighbouring half-graben basins, the syn-rift sedimentary record of the Bourg
462 d'Oisans Basin grades from thin and shallow marine platform deposits on fault block crests, to
463 thick and deeper (locally detrital) basinal deposits made of interbedded calcarenites and
464 hemipelagic to pelagic marls towards the master fault. Based on lithofacies and faunas, the
465 inferred maximum bathymetry of these European half graben depocenters was about 100-250
466 m. Their tectono-stratigraphic architecture revealed that they remained underfilled, an
467 interpretation supported by the local occurrences of olistoliths made of pre-rift and basement
468 rocks next to normal fault scarps. During the Sinemurian–Pliensbachian, rifting ceased
469 throughout the future proximal European margin, and the major rift faults were sealed. At that

470 time, depositional depths increased to 250–400 m in basins that record the subsequent
471 progradation of carbonate platforms from late to post-rift times (Chevalier, 2002).

472 ***The Il Motto Basin (Figs. 4d, 4e and 5b)*** was located at the former northern proximal Adriatic
473 margin. This basin is one out of several fault-bounded rift basins exposed in the Upper
474 Austroalpine Ortler Nappe (Eberli, 1988). It exposes a high-angle master fault bounded by a
475 half-graben extensional basin preserving the relationships between the pre-, syn- and post-
476 tectonic sediments (Eberli, 1987; Froitzheim, 1988; Conti et al., 1994; Ribes et al., 2019a). The
477 syn-tectonic sediments are made of Early Jurassic megabreccias that grade upsection and away
478 from the master fault into finer breccias and then calciturbidites. The megabreccias include
479 reworked carbonates sourced from the emerged and eroded pre-rift cover of the adjacent fault
480 scarp. It is important to note that the absence of clastic sedimentation implies that basement
481 rocks were never exposed and reworked at this stage in the syn-rift sediments. The syn-tectonic
482 sediments are interleaved with hemipelagic carbonates and shales dated as Early Hettangian to
483 Late Sinemurian (Furrer, 1985; Eberli, 1985; 1988). The master fault is sealed by ammonite-
484 bearing carbonates dated as Late Sinemurian to Early Pliensbachian. A younger marker
485 horizon, corresponding to the Toarcian Oceanic Anoxic Event (T-OAE; 183 Ma) occurs within
486 the post-tectonic sequence (Ribes et al. 2019a). Lithofacies, faunas and ichnofacies recorded in
487 background sediments indicate water depths in the range of 50–200 m during rifting, and deeper
488 conditions (several hundreds of meters) during the post-tectonic phase (Eberli, 1987). Thus, the
489 environments remained relatively shallow even after rifting, compared to the future distal
490 margins. The overall thinning- and fining-upward sequence is interpreted to reflect both an
491 aggradation-dominated setting (instead of a prograding fan), a progressive decrease of
492 redeposited sediments with respect to background sedimentation and a starvation of the
493 sedimentary system, most likely related to a deepening of the setting, and because the Adriatic
494 micro-continent became disconnected from continent-derived sedimentary sources (Eberli,
495 1987).

496
497 ***The Monte Generoso Basin (Figs. 4d, 4e and 5c)*** is one of several rift depocenters that have
498 been identified on the former southern Adriatic proximal margin. These depocenters formed
499 from Norian time onward; however, major normal faults began to separate half-graben and 30–
500 50 km wide horsts only during the Rhetian (Bernoulli, 1964; Bertotti et al., 1993). For the best-
501 investigated Monte Generoso Basin, Bertotti (1991) showed that its master fault (the Lugano-
502 Val Grande fault zone) penetrated basement and soled out at mid-crustal levels. Since the whole
503 domain has not been significantly thickened during Alpine convergence, the present crustal
504 thickness may not be much thicker than at the end of rifting. Thus, the Generoso Basin is likely
505 to have formed over a crust that was > 25 km thick. Rifting was linked to hemipelagic and
506 pelagic sequences, interleaved with calciturbidites, which were deposited with typical *half-
507 graben related, wedge-shaped* architecture. These sequences include spongolitic, calcarenite
508 and mud-rich turbidites with deepening upward facies, as well as megabreccias and olistoliths
509 in the vicinity of major fault scarps. Tectonic activity decreased drastically during the
510 Sinemurian and ceased during the Pliensbachian.

511 In summary, the syn-tectonic sedimentary record in the Bourg d'Oisans, Il Motto and Monte
512 Generoso Basins displays wedge-shaped deposits from latest Triassic to Sinemurian–
513 Pliensbachian time. In the temporal framework of the Alpine Tethys rifting, this corresponds to
514 the early syn-rift history referred to as *the stretching phase*. From Pliensbachian–Toarcian time

515 onward, the three basins and their surrounding proximal domains recorded passive infill, i.e.,
516 the upper part of the syn-rift has a post-tectonic depositional geometry. The proximal domains,
517 however, continued to subside but remained at relatively shallow water conditions, suggesting
518 that the underlying crust remained relatively thick, i.e., likely > 25 km.

519 **The necking phase recorded in the necking/distal domains (BB2 & BB3)**

520 The necking phase has been described in the Mont Blanc region (Ribes et al., 2020a) on the
521 European margin, in the Cusio–Arona region in the Southern Alps (Beltrando et al., 2015) and
522 in the Austroalpine Campo–Grosina nappe (Mohn et al., 2010). However, since there is no
523 sedimentary record in the latter, it will not be further described. All these domains are located
524 between the proximal and distal domains of the Alpine Tethys margins. The syn-rift
525 stratigraphy of the necking phase is also preserved in the Briançonnais domain near Briançon,
526 and at the Sostegno-Fenera region in the Biellese in Northern Italy. Below we discuss the syn-
527 necking evolution of the different sites.

528 **The Mont Blanc region (Figs. 4d, 4e and 6a)** has been interpreted to preserve the necking
529 domain of the former European margin (Masini et al., 2013; Ribes et al., 2020a). In contrast to
530 more proximal regions that display half-graben deposits, the syn-rift record of the necking
531 domain is more complex. The pre-rift (Triassic) and early syn-rift (Lower Jurassic) sediments
532 are either lacking, or are discontinuous and occur as allochthons. In the past, the lack of the pre-
533 and early syn-rift sediments was interpreted to result either from non-deposition, or from post-
534 depositional uplift and erosion. Where present, pre- and early syn-rift sediments were assumed
535 to represent the primary autochthonous sedimentary cover of the Mont Blanc Massif (Landry,
536 1978). More recently, Ribes et al. (2020a) emphasized that the basement of the Mont Blanc is
537 locally topped by pre-Alpine black gouges and cataclasites. They suggested that these rocks
538 indicate the presence of a major extensional detachment fault, which would be responsible for
539 the exhumation of the Mont Blanc granite and polymetamorphic basement to the seafloor. In
540 this interpretation, the Mont Blanc Massif corresponds to a core complex domal structure linked
541 to the tectonic creation of a new depositional surface, referred hereafter as “new real estate”.
542 The extensional detachment system has also been interpreted to be responsible for crustal
543 thinning (for examples see Mohn et al., 2012 and Ribes et al., 2020a). Exhumation is best
544 documented by early to mid-Jurassic siliciclastic sediments, the so-called *Grès Singuliers*.
545 These sediments rework the above-mentioned gouges/cataclasites and underlying basement,
546 and unconformably overlie the basement. Laterally, they overly conformably Lower Jurassic
547 carbonates (Ribes et al., 2020a). Note that the siliciclastic *Grès Singuliers* are surrounded by a
548 depositional setting that is dominated by carbonates (Trümpy, 1971). Nevertheless, the detrital
549 zircon provenance analysis reported in Ribes et al. (2020a) indicates that the *Grès Singuliers*
550 are locally sourced from the Mont Blanc and Aiguilles Rouges basement. Evidence for several
551 cycles of erosion and re-sedimentation within these deposits indicate a complex depositional
552 environment and explain the relative maturity of sandstones, despite the local sourcing. This is
553 in line with a significant tectonic exhumation and sub-aerial exposure of the local basement
554 during the necking phase. Additionally, sedimentary structures found in the *Grès Singuliers*
555 testify to a tidal influence, which further supports a shallow marine depositional environment
556 (Fig. 6a). The local siliciclastic source for the *Grès Singuliers* became inactive from the
557 Toarcian–Aalenian onward, either due to the cessation of the Mont Blanc extensional
558 detachment, and/or to the drowning of the European necking zone (Ribes et al., 2020a). The

559 overlying Middle- and Upper Jurassic syn-rift deposits are post-tectonic (i.e., deposited in a
560 non-tectonic setting; see Part 2 by Chenin et al., same volume, for definition and discussion of
561 syn-rift vs. pre/syn/post-tectonic). These post-tectonic deposits correspond to progradational
562 and aggradational carbonate platforms indicating that the area subsided, although the overall
563 crust remained thick enough to support shallow marine conditions on the proximal part of the
564 necking domain. In contrast, on the distal part, a major deepening is documented by the
565 occurrence of either thicker Upper Jurassic to Early Cretaceous post-rift sediments, or by the
566 occurrence of deep-water turbidites. A comparable situation can be found all along the external
567 massifs in the Western Alps.

568 **The Cusio–Biellese region (Fig s. 4d, 4e and 6c)** lies in Northern Italy at the transition between
569 the proximal and distal southern Adriatic margin. This region displays a complex syn-rift
570 stratigraphic record that was interpreted by Beltrando et al. (2015) and Decarlis et al. (2018) to
571 be linked to crustal necking. In this region, Sinemurian shallow-marine carbonates and
572 sandstones (the so-called San Quirico Sandstone) unconformably overlie a karstified Triassic
573 platform in the west (Sostegno and Fenera) and basement in the east (Gozano and LAVORIO;
574 Berra et al., 2009; Beltrando et al., 2015). The analysis of the San Quirico Sandstone indicates
575 that it has been sourced from a local basement (Permian volcanic rocks and Variscan
576 metamorphic basement), suggesting basement emersion in the Cusio–Biellese region. The
577 occurrence of zircon grains with fission track ages of 177 ± 6 Ma in the San Quirico Sandstone,
578 with a depositional age of Late Pliensbachian to Toarcian (~ 182 Ma), suggests that the
579 deposition of this sandstone was contemporaneous with basement exhumation (Beltrando et al.,
580 2015). This observation is similar to observations made in the *Grès Singuliers* at Mont Blanc
581 (see previous section; Fig. 6a) and suggests that the Cusio–Biellese region necking may also
582 have been linked with the development of extensional detachment faults and core complex
583 structures. Although such structures have not yet been identified in the Cusio–Biellese region
584 due to poor exposure, the fission track ages suggest tectonic exhumation associated with erosion
585 (Decarlis et al., 2018). The surrounding depositional environment remained shallow-marine,
586 and no coeval sub-aerial uplift of the more proximal parts are reported during the necking stage,
587 ruling out the possibility of long-wavelength dynamic topography (Flament et al., 2013). It is
588 also important to note that the whole domain is sealed by post-tectonic carbonates of
589 Pliensbachian age (Berra et al., 2009; Decarlis et al., 2017). This shows a complex stratigraphic
590 record of the syn-necking depositional sequence. This sequence is characterized by an
591 unconformable base and a conformable boundary with the overlying post-tectonic sediments.

592 **The Briançonnais domain (Fig s. 4d, 4e and 6b)** belongs to the distal part of the European
593 margin. During the necking stage, this domain was part of the keystone (H-block) before its
594 delamination and fragmentation between the two margins (Lavie & Manatschal, 2006; Masini
595 et al., 2013; Hauptert et al., 2016). Restorations of this domain suggest that it was several tens
596 of kilometres wide and extended over several hundred kilometres along strike. Early Jurassic
597 emersion is documented by a regional unconformity and karstification of pre-existing shelf
598 carbonates, resulting in a major, regional, syn-rift stratigraphic gap (De Graciansky et al., 2011).
599 This stratigraphic unconformity contrasts with the continuous sedimentary record of the
600 adjacent areas, which were subsiding at this time (Claudel & Dumont, 1999; Decarlis & Lualdi,
601 2008). The onset of emersion occurred at the earliest during the Sinemurian, which is the age
602 of the youngest marine carbonates affected by the karst (Tricart et al., 1988). Drowning of the
603 Briançonnais domain started at the latest during the late Bathonian (~ 165 Ma), since shallow

604 marine carbonates of this age locally overlie the karst (Claudel & Dumont, 1999). Due to the
605 existence of widespread pelagic limestones of Callovian age (~164–161 Ma) draping the entire
606 Briançonnais domain, rapid drowning and deepening was commonly assumed (e.g., Claudel &
607 Dumont, 1999; De Graciansky et al., 2011). More recently, however, Hauptert et al. (2016)
608 suggested that drowning may have started earlier but was not recorded because passive infill
609 was restricted to the lows on either side of the Briançonnais High. The pelagic nature of the
610 sediments draping the Briançonnais domain does not necessarily indicate a fast subsidence
611 and/or a deep water, since pelagic sediments can be deposited in relatively shallow water depth
612 (below wave base) on isolated highs disconnected from sedimentary sources. The regionality
613 of the Jurassic karst, and the consistent nature and age of the overlying sediments, suggest that
614 both emersion and drowning were, from a geological timescale perspective, largely
615 synchronous over the entire Briançonnais domain and occurred during the necking phase.

616 In summary, the observations from the Mont Blanc Massif and the Cusio–Biellese region and
617 the Briançonnais domain show that: 1) the base of the syn-tectonic sequence is conformable
618 over the proximal domain, whereas it is unconformable in the necking domain where core
619 complexes formed (e.g., new real estate over the necking domain) and over the syn-rift karst
620 capping the Briançonnais High (BB3); 2) the necking domains and the keystone (H-block)
621 between them were local regions of either siliciclastic deposits (sandstones) due to local sub-
622 arial exhumation of basement rocks going along with erosion/deposition, or karstification of
623 the pre-rift carbonate platform; 3) water-depth remained relatively shallow during the necking
624 phase and the thickness of related syn-tectonic sediments is therefore limited; and 4) the
625 transition into the overlying post-tectonic sediments is conformable where sedimentation rates
626 remained high, and unconformable where starvation occurred due to the fast subsidence post-
627 dating necking.

628 **The hyperextension phase exposed in the distal domains (BB4, BB5 and BB6)**

629 Exposures of the former hyperextended and exhumed mantle domains of the European margin
630 occur in the Sub-, Lower- and Middle Penninic nappes, and the Pre-Piemonte units, which are,
631 except the Tasna OCT (Ribes et al. 2020b), strongly overprinted by Alpine deformation. In
632 contrast, the distal domains of the former Adriatic margin are much better preserved and are
633 exposed in the Lower Austroalpine Err and Bernina Nappes, and the South Penninic Upper
634 Platta Unit (Epin et al., 2017). In the western Southern Alps, there are some exposures in the
635 Canavese Zone that may represent remnants of the former hyperextended margin (Beltrando et
636 al., 2014; Decarlis et al., 2017). Due to the complex, segmented margin architecture, the along-
637 strike distribution of the hyperextended domain is complex, in particular along the European
638 distal margin. For instance, former studies suggested that the Valais Basin formed during
639 Cretaceous rifting, simultaneous with the Bay of Biscay (Frisch, 1979; Stampfli, 1993; Handy
640 et al., 2010), despite a Jurassic age of the basin was already proposed by Steinmann (1994) (for
641 details see Pfiffner, 2014). A Jurassic age for the Valais Basin is supported by the syn-tectonic
642 sediments in this basin that are Middle Jurassic and mantle exhumation dated late Middle
643 Jurassic (Ribes et al. 2020b). In this study we propose that the Valais Basin formed as a
644 segmented, en-echelon, hyperextended basin simultaneous with the Ligurian and Piemonte
645 basins. In a subsequent stage (after the late Middle Jurassic) these basins connected, giving
646 birth to the Alpine Tethys proto-oceanic domain (for paleogeographic evolution see Fig. 4).

647 **The Tasna OCT (Figs. 4d, 4e and 7a)** exposes a well-preserved relict of the most distal part of
648 the European margin (western edge of the Briançonnais continental ribbon) and its transition
649 into the exhumed mantle domain of the former Valais Basin (Trümpy, 1980). The Tasna Nappe
650 was intensively studied by Florineth & Froitzheim (1994), Manatschal et al. (2006), and more
651 recently revisited by Ribes et al. (2020b). The Tasna OCT preserves upper- and lower, pre-rift
652 continental crust that is juxtaposed along an extensional detachment, the Upper Tasna
653 Detachment. It is noteworthy that middle crustal material is missing in this section (Ribes et al.
654 2020b). Continent-wards (i.e., towards the Briançonnais in this area), a stratigraphic interface
655 can be defined between the upper crust, made of a polymetamorphic Variscan basement, and
656 pre-rift Triassic dolostones, and Lower Jurassic syn-rift limestones. This succession is part of a
657 block that is interpreted to represent an extensional allochthon (e.g., Fig. 4 in Ribes et al.
658 2020b). Oceanwards (i.e., towards the north), the top basement is strongly tectonized and
659 covered with tectono-sedimentary breccias including clasts of Triassic dolomites and of the
660 underlying, exhumed basement. Top basement is therefore interpreted as a detachment fault
661 surface (Ribes et al., 2020b). Two main detachment faults have been identified: the Upper
662 Tasna Detachment between the lower crust and upper crust, or lower crust and syn-tectonic
663 sediments where the upper crust is lacking; and the Lower Tasna Detachment between mantle
664 and the base of the lower crust, or the mantle and syn- or post-tectonic sediments where the
665 mantle was exhumed to the seafloor (Florineth & Froitzheim, 1994). The first post-tectonic
666 sediments deposited onto the syn-rift tectono-sedimentary breccias throughout the Tasna OCT
667 are dark shales. They are locally interbedded with sandstone beds that also seal the allochthon
668 block located further south in the section. The syn-tectonic sediments are interpreted to be late
669 Lower Jurassic to Upper Jurassic (Ribes et al., 2020b). This is in line with Ar/Ar cooling ages
670 yielding an age of 170.5 ± 0.4 Ma obtained from phlogopites. These phlogopites are derived from
671 a spinel websterite from within the mantle lying in the footwall of the Lower Tasna Detachment
672 (Manatschal et al., 2006, see also the discussion in Ribes et al. 2020b).

673 In the nearby Falknis nappe, which has been interpreted to sample the continent-ward
674 continuation of the Tasna OCT (i.e., the Briançonnais platform), massive breccias interfinger
675 with syn-rift sediments in the Tasna OCT, and are therefore interpreted as contemporaneous
676 (Ribes et al., 2020b). These breccias were interpreted to reflect the long-lasting existence of a
677 mega-fault scarp that is characteristic for an upper-plate margin (e.g., BB5; Ribes et al. 2019b).
678 The breccias are also interlayered with a starved sediment horizon, comprised of radiolarian
679 cherts, which marks the termination of rifting. It also suggests deep depositional environments
680 (below the Carbonate Compensation Depth) at the end of rifting in the Tasna OCT.

681 **The Bernina and Err Nappes (Figs. 4d, 4e and 7b)** preserve the most distal part of the North-
682 Adria margin. The Err Nappe was the first place in the Alps where rift-related detachment faults
683 were discovered (Froitzheim & Eberli, 1990). The Err detachment system was subsequently
684 studied by Manatschal & Froitzheim (1996), Manatschal & Nievergelt (1997), Masini et al.
685 (2011, 2012), Epin et al. (2017) and Epin & Manatschal (2018). A second major detachment
686 system has been described in the Bernina nappe and was referred to as the Bernina detachment
687 system (Mohn et al., 2011, 2012). The Err detachment system is made of at least four, in-
688 sequence detachment faults (namely the Err, Jenatsch, Agnel and Upper Platta detachment
689 faults), whose length and size of associated breakaway blocks decrease oceanward (Epin &
690 Manatschal, 2018). The last detachment is responsible for mantle exhumation exposed in the
691 Upper Platta Unit. The detachment faults are characterized by diagnostic black gouges and
692 green cataclasites (Manatschal, 1999), which separate the massive, little deformed but hydrated

693 basement (continental crust or subcontinental mantle) in the footwall either from allochthonous
694 blocks of continental crust and/or pre-rift sediments, or from late syn- to post-rift sediments
695 (Masini et al., 2012). These detachment faults reached the seafloor at low angles ($< 15^\circ$), as
696 shown by the low angle between the exhumation surface and the overlying sediments (Epin &
697 Manatschal, 2018; Fig. 7b). The lack of quartz mylonites along the detachment fault suggests
698 that deformation occurred in the brittle regime, at relatively low temperature ($< 300^\circ\text{C}$;
699 Manatschal, 1999). Crustal basement exhumed in the Err Nappe corresponds to pre-rift upper
700 crust, pre-rift lower crust has not been reported so far.

701 The Err detachment system is characterized by a discontinuous record of pre-rift sediments,
702 complex, discontinuous syn-tectonic sedimentary deposits, and continuous post-rift sediments
703 (Masini et al., 2012; Epin et al., 2017; Ribes et al. 2019a). The tectono-stratigraphy of the syn-
704 tectonic sediments is well preserved in the so-called Samedan Basin (Masini et al., 2011, 2012;
705 Epin & Manatschal, 2018). In this basin, pre-rift sediments are only found as allochthonous
706 blocks overriding a detachment fault (e.g., Bardella allochthon; Fig. 7b). Based on structural
707 and stratigraphic relationships, and structural restorations of Alpine sections, Masini et al.
708 (2011) suggested that the Samedan Basin initiated as a classical half graben basin. Continued
709 extension on the high-angle fault led to its flattening and to the exhumation of deeper basement
710 levels. At this stage, the initial high-angle fault had become an extensional detachment fault
711 whose inactive portion lied at a low-angle to the seafloor. In such an example, the syn-tectonic
712 sediments were deposited directly onto exhumed basement (new real estate). Those sediments
713 are composed of siliciclastic, basement-derived, immature and locally derived breccias that
714 directly overlie the detachment system (e.g., member A of the Saluver Fm. of Finger et al.,
715 1978). In contrast, the sediments near the hanging wall block are exclusively made of carbonate
716 breccias sourced from the adjacent allochthonous block (e.g., Bardella Fm.; Fig. 7b). The
717 different composition of the coeval early syn-tectonic sediments have been interpreted to reflect
718 a change from hanging wall-derived breccias composed of Triassic pre-rift carbonate clasts to
719 footwall-derived breccias made of basement clasts as the result of the exhumation of basement
720 rocks along the detachment fault flooring the basin (Masini et al., 2011). These sediments are
721 overlain by a succession of fining- and thinning-upward turbiditic deposits that grade upwards
722 into hemipelagic sediments and radiolarian cherts, recording sediment starvation and deepening
723 of the basin once detachment faulting locally stopped (for details see Masini et al., 2011).

724
725 ***The Canavese zone*** in northern Italy preserves remnants of the distal part of the South-Adria
726 margin. Although the sedimentary record of the Canavese zone is poorly exposed and was
727 largely dismembered during the Alpine orogeny, its similarity with that of the Err nappe
728 prompted Ferrando et al. (2004) to interpret it as an equivalent distal part (hyperextended
729 domain). It was subsequently studied by Decarlis et al. (2013) and Beltrando et al. (2015).
730 Recently, Decarlis et al. (2017) suggested, based on tectono-stratigraphic and paleo-
731 geomorphological studies, that the Canavese zone belongs to an upper plate margin, and thus
732 that it would be more comparable with the Tasna OCT. The Canavese displays two types of
733 exhumed basement: an amphibolite-grade basement with shallow intrusions of Permian
734 granitoid, interpreted as pre-rift upper crust; and a migmatitic basement with mafic granulite
735 intrusions, recognized as a pre-rift lower crust (Ferrando et al., 2004). The Middle Jurassic syn-
736 tectonic sedimentary deposits include both matrix-supported breccias dominated by basement
737 clasts and matrix-supported breccias rich in Triassic dolostone clasts. Both facies overly
738 tectonized, exhumed basement covered with tectono-sedimentary breccias (Ferrando et al.,

739 2004). Middle Jurassic breccias are overlain by Middle- to Late Jurassic radiolarian cherts (Bill
740 et al., 2001). Thus, the overall observations show similarities to the Tasna OCT.

741 In summary, Falknis-Tasna and Err-Bernina display a comparable tectono-sedimentary record
742 controlled by extensional detachment faults. While Err-Bernina belong to a lower plate margin,
743 Falknis-Tasna are part of an upper plate margin (Fig. 7c). However, it is important to note that
744 these sites were not conjugate although they may have belonged to the same margin segment
745 (Fig. 4). All sites presented here display: 1) dismembered pre-rift and early syn-rift sediments
746 only preserved in allochthonous and breakaway blocks; 2) exhumed basement along
747 extensional detachment faults overlain by syn-tectonic tectono-sedimentary breccias containing
748 clasts of the underlying exhumed basement; 3) evidence for deepening and starvation, which
749 we here link to the hyperextension phase. Apart from these similarities, there are also some
750 differences. In the Bernina-Err example (Figs. 7), which belongs to a lower plate margin (Epin
751 & Manatschal, 2018), detachment faults cut from the upper crust directly into mantle and the
752 lower crust is missing. In contrast, at the upper-plate margins (e.g., Tasna OCT and Canavese),
753 lower crustal rocks are exhumed (Fig. 7c).

754 **The proto-oceanic domains of the Alpine Tethys (BB7)**

755 Remnants from the proto-oceanic domain are found all along the Alpine belt in the South
756 Penninic units that constitute the Alpine suture (Fig. 1c). The best-preserved exposures of the
757 proto-oceanic domain, that escaped subduction and a related high-pressure metamorphic
758 overprint, are exposed in the Lower Platta Unit in SE-Switzerland and in the Chenaillet
759 Ophiolite in the French-Italian Alps (Fig. 8).

760

761 ***The Lower Platta unit (Figs. 4d, 4e and 8a)*** belongs to the south Penninic units exposed in SE-
762 Switzerland. It samples an exhumed mantle domain that includes magmatic additions. This
763 domain can be restored back to the northern Adriatic distal margin. It was extensively studied
764 by Dietrich (1969), Manatschal & Nievergelt (1997), Desmurs et al. (2001, 2002), Schaltegger
765 et al. (2002), Müntener et al. (2004), and more recently by Epin et al. (2017, 2019), Coltat et al.
766 (2019a, 2019b, 2020) and Amann et al. (2020). The Platta Nappe can be subdivided into two
767 units based on their lithology, namely the Upper- and Lower Platta Units (Desmurs et al., 2002)
768 (Fig. 8c). The Upper Platta Unit corresponds to the most proximal part of the exhumed mantle
769 domain. It is comprised of inherited subcontinental lithospheric mantle with minor magmatic
770 additions, and a few overlying continental allochthons. In this study, we consider it as part of
771 the hyperextended domain (Epin & Manatschal, 2018). In contrast, the more distal Lower Platta
772 Unit is made of (re-)fertilized mantle, i.e., a mantle that reacted with percolating magma (for
773 details see Müntener et al., 2004), with an increasing volume of intrusive and extrusive
774 magmatic bodies oceanward (Fig. 8c). It also preserves remnants of a proto-Oceanic Core
775 Complex (OCC; Epin et al., 2019). The entire exhumed mantle domain is characterized by
776 intense hydrothermal fluid activity and precipitation of metalliferous mineralization (Coltat et
777 al., 2019a, 2019b). Extensional structures found in the lower Platta Unit are characterized by
778 polyphase extensional detachment faults, truncated by late, high-angle normal faults (Fig. 8c;
779 Epin et al., 2019; Coltat et al., 2020). They include serpentinite cataclasites and serpentinite
780 gouges, topped by ophicalcites and overlain by tectono-sedimentary breccias, which are typical
781 fingerprints of Jurassic detachment faults (Epin et al., 2017). An idealized section through the
782 footwall of a Platta detachment fault includes, from base to top (see Fig. 8a section 1): (1)

783 foliated massive serpentized peridotite or gabbro; (2) serpentized peridotite or gabbro
784 cataclasites marked by fractures and veins filled with syn-kinematic chlorite and serpentinite;
785 the intensity of cataclastic deformation increases upward, passing into (3) serpentinite gouges
786 (fault core).

787 The first sediments overlying the detachment surface are tectono-sedimentary breccias and
788 ophicalcites (see section 3 in Fig. 8a; Desmurs et al., 2001; Epin et al., 2019). The latter form
789 in a post-exhumation stage at low temperature (< 100–150°C), except where they are overlain
790 by basalts resulting in higher formation temperatures (see section 2 in Fig. 8a; Coltat et al.,
791 2020). The next sedimentary sequence (see Fig. 8b sections 2 and 3) is made of red clays and
792 radiolarian cherts that include also hydrothermal cherts and reworked, continent-derived
793 material. These sediments are dated Bajocian to Kimmeridgian in the Alpine Tethys (Bill et al.,
794 2001; Baumgartner, 2013). The upper part of the radiolarian cherts overlies, and thus post-dates
795 the basalts and tectono-sedimentary breccia in the exhumed mantle domain. The basalts that
796 show a T-MOR composition (Desmurs et al., 2002), also referred to as OCT basalts by Amann
797 et al. (2020), have been interpreted to be syn-tectonic based on the observation of basalts
798 thickening into high-angle faults and basalts that are deformed during mantle exhumation (Epin
799 et al., 2019; Coltat et al., 2020) (see also sections 2 and 3 in Fig. 8b).

800

801 ***The Chenaillet Ophiolite (Figs. 4d, 4e and 8b)*** displays pillow lavas with a MORB signature
802 overlying mafic plutonic rocks and serpentized subcontinental mantle (Mantle type 2, i.e.,
803 refertilized mantle of Picazo et al., 2016). The first tens to hundreds of meters of the exhumed
804 mantle are affected by brittle deformation and pervasive hydrothermal circulation. Pillow lavas
805 are undeformed, implying they were emplaced after mantle exhumation, during a subsequent
806 phase of high-angle normal faulting (Manatschal et al., 2011) (see observation at Cima le Vert;
807 Fig. 8b). Manatschal et al. (2011) suggested that these faults served as feeder channels for the
808 extrusives. The first observed sediments overly the exhumed mantle and/or intrusive mafic
809 rocks (see observation at La Loubatière; Fig. 8b). They include breccias, graded sandstones and
810 siltstones that are exclusively made of mantle-derived materials, and to a lesser extent gabbro-
811 and continent-derived material. Rare basaltic clasts are found in these sediments, which were
812 emplaced by gravitational processes over the exhumed mantle. This implies formation of
813 topography during mantle exhumation similar to present-day OCC at mid ocean ridges
814 (MacLeod et al., 2009). At the Chenaillet Ophiolite, syn-magmatic sediments are rare, apart
815 from hyaloclastites and subordinate siliciclastic sediments that are interbedded within the
816 volcanic sequence (Masini, pers. com). No younger, Upper Jurassic to Upper Cretaceous post-
817 rift sediments are described.

818 In summary, the tectono-sedimentary record of the Lower Platta Unit and the Chenaillet
819 Ophiolite, both preserving remnants of proto-oceanic crust, shows that: (1) mantle exhumation
820 was achieved via slip on successive extensional detachment faults later affected by high-angle
821 normal faults; (2) topography was created during mantle exhumation and resulted in
822 gravitational sedimentation; (3) the late normal faults may have served as feeder channels for
823 the overlying volcanic sequences; (4) no pre-rift or early syn-rift deposits exist in the exhumed
824 mantle domain; and (5) the first syn- to post-magmatic sedimentary deposits (radiolarian cherts)
825 show the importance of fluids (hydrothermal cherts), reworking (distal turbidites and/or
826 contourites), and pelagic sedimentation (radiolarites).

827 **READING THE TECTONO-STRATIGRAPHIC TAPE RECORDER OF**
828 **THE ALPINE TETHYS**

829 **A Wheeler diagram for the Alpine Tethys margins**

830 In this section we describe the syn-rift mega-sequence within a margin-scale Wheeler diagram,
831 which is an excellent tool to represent the tectono-sedimentary evolution during the entire rift
832 event (Fig. 9). Ribes et al. (2019a) subdivided the syn-rift mega-sequence into four tracts, the
833 stretching-, necking-, hyperextension-, and proto-oceanic tracts. In order to compare our results
834 to seismic sequences from present-day rifted margins, we use here tectonic sequences (TS) that
835 replace the “tracts” terminology previously proposed (for definition and discussion of TS, see
836 accompanying paper by Chenin et al., same volume). Each TS encompasses all the sediments
837 deposited during the period of activity of the corresponding rift phase. Thus, it represents a
838 chronostratigraphically significant package of sediments related to a distinct phase of the basin
839 evolution. Each TS includes syn- and post-tectonic packages that are diachronous along the
840 margin, the former linked to faults, the later sealing faults or showing passive infill of rift-
841 related relief. Using this approach allows us to describe the sedimentary development during
842 rifting and to link the kinematic evolution to sediment deposition. This approach relies on the
843 stratigraphic tape recorder to describe the evolution of rifting from incipient rifting to final
844 break-up. The first prerequisite is that sediments can be attributed to a specific rift domain, a
845 second is that a time frame for the different rift events, faults, TS, and magmatic additions can
846 be defined. However, in contrast to present-day margins where timelines (reflective horizons in
847 a reflection seismic section) can be followed from the proximal towards the distal parts, in the
848 case of the Alps, this time frame is more difficult to establish. For the Grischun transect (Fig.
849 3b), Ribes et al. (2019a) proposed global or regional events that can be used as timelines to
850 correlate across the margin. These lines are the Rhaetian (base of the syn-rift sequence,
851 ~200Ma), the Toarcian Oceanic Anoxic Event (~185Ma), the Bajocian-Bathonian bio-Siliceous
852 Event (~165Ma) and the Tithonian Carbonate Event (~155Ma). It is, however, important to
853 note that the tectonic events are not necessarily synchronized with these time markers.

854 In this paper, we use the following ages for the successive rift phases in the Alpine Tethys
855 domain that are based on the studies of Masini et al. (2013) and Ribes et al. (2019a): 200 ± 5 Ma
856 for onset of rifting, 185 ± 5 Ma for necking; 175 ± 5 Ma for onset of hyperextension along the
857 distal margin, 165 ± 5 Ma for onset of tectono-magmatic accretion in a proto-oceanic domain.
858 Ages may in fact differ between the various rift segments of the Alpine Tethys. Here we mainly
859 refer to the central, i.e., the Piemonte segment. It is important to note that the age of onset of
860 hyperextension is ill-defined. Note also that we define only the onset of mantle exhumation, but
861 not the onset of seafloor spreading, since in the Alpine Tethys there is no direct evidence for
862 steady-state seafloor spreading.

863 Apart from the time frame, we also need to insist on the definition of syn-rift vs. syn-tectonic
864 that is exemplified within our Wheeler diagram. Syn-rift corresponds to the time between onset
865 and end of rifting, in our example between 200 ± 5 Ma and 165 ± 5 Ma (Fig. 9). Syn-tectonic
866 corresponds more specifically to a sedimentary sequence that is deposited during extension and
867 involving syn-fault deposition. In contrast, pre-tectonic and post-tectonic refer to sediments that
868 are deposited during the syn-rift time interval, but that precede or post-date active faulting in a
869 given place. Another important notion introduced already before, but fundamental to the
870 understanding of the Wheeler diagram shown in Fig. 9, is the concept of “*new real estate*”. It

871 refers to newly created surfaces offered to potential deposition, which are either due to tectonic
872 exhumation along extensional detachment faults or related to accretion of new oceanic crust.
873 Introducing “new real estate” is a major modification to the classical Wheeler diagrams used in
874 basin analysis, and has major implications for the description of the time-space relation between
875 the stretching, necking, hyperextended and proto-oceanic tracts (for more details see Chenin et
876 al. this volume). In the Wheeler diagram shown in Fig. 9, we also represent the seven BBs. For
877 the proto-oceanic tract, we also include the extrusive magmatic additions that were the main
878 syn-tectonic depositional sequence.

879 **Linking the tape recorder with the rift evolution**

880 Rift onset in the western Tethys realm is difficult to define, since rifting nucleated in different
881 areas at different times: in the east and south (Meliata/Vardar) during the Permo-Triassic, in the
882 Alpine Tethys at the end of Triassic, and in the southern North Atlantic/Pyrenean domain in the
883 Late Jurassic-Early Cretaceous (Figs. 1b and 4). In this study we focus on the Alpine Tethys
884 and more precisely, the Piemonte segment.

885 During the stretching phase (latest Triassic to late Sinemurian/early Pliensbachian: 200 ± 5 to
886 185 ± 5 Ma), extension was distributed over a wide area, i.e., from the Cevennes in France to
887 the Trento-plateau in Northern Italy, with the development of many half-graben/graben (e.g.,
888 Bourg d’Oisans, Generoso and Il Motto Basins; Fig. 10d). All these depocenters were bounded
889 by listric normal faults that were at a high angle in the upper crust and are interpreted to sole
890 out in the middle ductile crust (see Bertotti, 1991). The total amount of extension
891 accommodated during this event may have been minor. Considering the Alpine Tethys, Bertotti
892 et al. (1993) calculated β values of 1.22 for this stage. Even if some basins may have
893 accommodated several kilometres of syn-tectonic sedimentary deposits, the overall crustal
894 thinning remained moderate and widely distributed.

895 The necking phase initiated during the late Sinemurian to early Pliensbachian (185 ± 5 Ma). It
896 was associated with the cessation of distributed extension, local uplift of the future distal
897 domain, and subsequent localization of extension and fast subsidence (Fig. 10c). This evolution
898 resulted in a complex stratigraphic record of the necking stage recorded by the necking TS.
899 Local uplift, some few hundreds of meters at maximum, and first occurrence of exhumation
900 faults on both sides of a keystone (H-Block) resulted in major unconformities that are recorded
901 at the transition between the proximal and future distal margins (Mont Blanc at the European
902 margin and Cusio–Biellese and Campo-Grosina at the Adriatic margin). Uplift of the domain
903 in-between, the so-called Briançonnais domain, can also be observed, resulting in a major
904 unconformity that can be mapped along the margin and that is of necking age. Numerical
905 modelling suggests that necking-related uplift occurs when the upper lithospheric mantle,
906 considered as the strongest layer within the lithosphere, yields beneath a little-thinned
907 continental crust (Chenin et al., 2019, 2020). This event is followed by a flexural rebound that
908 can potentially lead to the emersion of formerly marine regions. In the Alps, this event occurred
909 after the Late Sinemurian and before the Toarcian, i.e., most likely during the Pliensbachian
910 (185 ± 5 Ma). As a consequence, the base of the necking TS is characterized by a conformable
911 contact over the proximal domain that seals the stretching phase faults, and an unconformable
912 contact over the future distal parts of the margin (for example see the Bardella allochthon, Fig.
913 7b). The top is either conformable or, in sediment-starved margins like the Alpine Tethys,
914 paraconformable due to a delayed passive infill (onlaps on rift-related residual topography).

915 The hyperextension phase (Fig. 10b) is well documented in the Lower Austroalpine Err and
916 Bernina Nappes, which belong to the distal northern Adriatic margin, and in the Tasna OCT,
917 which belong to the distal European margin. These domains are formed by a crustal wedge that
918 is interpreted to taper to zero due to the action of in-sequence extensional detachment faults
919 that propagate towards the future site of breakup. Hyperextension was the only rift phase during
920 which deformation was clearly asymmetrical, resulting in an upper and a lower plate margin.
921 At this stage, the entire rifted area was subsiding. While the proximal parts, which were
922 tectonically inactive, subsided thermally, the distal parts are interpreted to have subsided due
923 to a combination of crustal thinning (tectonic subsidence) and thermal equilibration (thermal
924 subsidence). The successive in-sequence detachment faults that developed during the
925 hyperextension phase rooted in the mantle and eventually led to the exhumation of mantle to
926 the seafloor (Fig. 10b). Hyperextension and mantle exhumation occurred during and after the
927 Toarcian anoxic event, but before the deposition of the radiolarian cherts, namely in the 180 to
928 165 Ma time interval. Sedimentation occurred simultaneous to fast subsidence, resulting in a
929 general deepening of the depositional environments. While in the lower plate margin breccias
930 are mainly linked to exhumation faults flooring the hyperextended basins, the upper plate
931 margin shows massive breccia-bodies linked to long-lived mega-fault scarps lying between the
932 residual keystone block (BB3) and the hyperextended domain (BB5) (Ribes et al. 2019b; Figs.
933 3a and 7c).

934 The proto-oceanic phase (Fig. 10a) initiated with the first extrusion of magma that post-dates
935 initial mantle exhumation. Both are intimately related with extensional faulting (detachment
936 and high-angle normal faults) and hydrothermal activity. Recent studies show that the first
937 exhumed mantle at the tip of a magma-poor margin is the subcontinental lithospheric mantle
938 that was underlying the pre-rift continental crust (mantle-type 1 of Picazo et al., 2016). In more
939 advanced stages of exhumation, deeper parts of the subcontinental mantle can be exhumed
940 (mantle-type 2 of Picazo et al., 2016). This type of mantle shows two important features: i) it
941 was depleted; i.e., it melted during the Permian (e.g., Rampone et al., 1998; Müntener et al.,
942 2004; McCarthy & Müntener, 2015) and/or showed inherited depleted heterogeneities
943 (Tribuzio et al., 2004; Sanfilippo et al., 2019); and ii) it was infiltrated by magma during
944 subsequent rifting (e.g., Rampone et al., 1997, 2020; Piccardo *et al.*, 2004, 2007; Müntener et
945 al., 2010). In the Alpine Tethys, mantle exhumation was associated with minor magmatic
946 activity, sometimes interpreted as embryonic seafloor spreading (Manatschal & Müntener,
947 2009; Manatschal et al., 2011; Epin et al., 2019; Jagoutz et al., 2007; Lagabrielle et al., 2015).
948 The magma-poor nature of the Alpine Tethys OCT may have originated due to Permian
949 depletion (Chenin et al., 2017), which was linked to a massive magmatic event throughout
950 Western Europe following the Variscan orogenic collapse (Bonin et al., 1998; Petri et al., 2017
951 cum references). The Jurassic rift-related infiltration may have been protracted, with a
952 magmatic plumbing system that built from the base of the lithosphere to the top. It is assumed
953 to have initiated with asthenospheric melt infiltration at ca. 185 Ma and to have reached the
954 surface with first magma extrusions (basalts) and shallow intrusions (gabbros) at about 165 Ma
955 (Desmurs et al., 2001, 2002; Schaltegger et al., 2002). Recent studies on the first basalts (Renna
956 et al., 2018; Amann et al., 2020) showed a complex magmatic evolution during the mantle
957 exhumation phase, partially controlled by the inherited mantle lithosphere composition. At
958 present, there is no evidence that the Alpine Tethys developed a mature, steady-state spreading
959 system (Picazo et al., 2016). The radiolarian cherts that are dated from Bajocian to
960 Kimmeridgian (Bill et al., 2001) were deposited during the accretion of the proto-oceanic

961 domain. These sediments formed at deep marine conditions below the calcite compensation
962 depth and are time equivalent to pelagic, but not necessarily very deep sediments on the more
963 proximal parts of the sediment-starved Adriatic microcontinent.

964 **Rift phases and their stratigraphic record**

965 Observations from the Alpine Tethys presented in this paper clearly show that the syn-rift
966 stratigraphic record is complex and cannot be explained by the simple, monophasic rift model
967 proposed by McKenzie (1978). The Alpine Tethys stratigraphic tape recorder shows evidence
968 for an abrupt switch from distributed (stretching) to localized (necking) deformation during the
969 Sinemurian/Pliensbachian (185 ± 5 Ma). In contrast, precisely identifying the transition from
970 necking to hyperextension in time and space is difficult in the Alpine system, while the
971 transition is spatially well defined at present rifted margins where the crust is thinned to less
972 than 10 km and the whole crust is in the brittle domain (Sutra et al., 2013; Nirrengarten et al.,
973 2016). Pinto et al. (2015) showed that a characteristic of the hyperextension phase is the
974 occurrence of mantle-derived fluids percolating faults and sediments and leaving a geochemical
975 signature. Another major switch occurs when magma becomes the dominant phase, which in
976 the Alpine Tethys occurs in the Bathonian to Callovian (165 ± 5 Ma) and coincides with the
977 proto-oceanic phase.

978

979 *Link between rift phase and tectonic sequences*

980 A major conclusion of this paper is that each of the four rift phases results in a distinct syn-
981 tectonic sedimentary record and can be described by the four successive stretching-, necking-,
982 hyperextension- and proto-oceanic TS (see also accompanying paper by Chenin et al. this
983 volume). The reason is that during each phase accommodation is created in a different way
984 (Fig. 10). The stretching TS is linked to the accumulation of sediments showing characteristic
985 syn-tectonic, wedge-shaped architectures in distributed fault-bounded basins (Fig. 10d). The
986 subsequent necking, hyperextension and proto-oceanic TS (Figs. 10c to 10a) have been little
987 investigated so far, but show diagnostic features reflecting their distinct structural and isostatic
988 evolution. The necking phase is characterized by a localization of extension simultaneous to
989 local uplift of a keystone and along hinge zones, and formation of exhumation faults at both
990 extremities, shortly followed by fast subsidence. As a consequence, the necking tract has an
991 unconformable base, accommodation is controlled by the interplay of detachment faults and
992 uplift/subsidence in disconnected and transient depocenters, and its top is conformable if
993 sedimentation rates are high. The hyperextension tract forms in a rapidly subsiding basin during
994 in-sequence stepping of extensional detachment faults towards the site of future breakup. As a
995 consequence, this tract is post-tectonic over the future proximal margins, the syn-tectonic
996 sequence is stepping ocean-wards on the lower plate but remains stationary over the location of
997 exhumation in the upper plate. Horizontal accommodation results from the formation of new
998 real estate and vertical accommodation from rapid subsidence. This combination of the
999 simultaneous creation of vertical and horizontal accommodation results in banana-shaped
1000 sequences often referred to as “sag” basins in the present-day hyperextended magma-poor rifted
1001 margins. The proto-oceanic TS is more complex, often sediment-starved, and includes syn-
1002 tectonic magma emplacement. The most characteristic observation is that of flip-flop faults
1003 create highs and lows, which lows becoming highs during subsequent stages. This explains two

1004 main observations: 1) detachment faults are truncated by younger high-angle faults, and 2) the
1005 occurrence of breccias and debris flows at the break away of younger faults, i.e., over highs.

1006 *Link between deformation and the syn-rift stratigraphic record*

1007 A key in controlling the way accommodation is created (i.e., horizontal vs. vertical) is the
1008 geometry of faults. This geometry depends on the bulk crustal/lithospheric rheology, which in
1009 turn controls the strain localization, and hence shape and width of crustal necking zones (Chenin
1010 et al., 2018b). However, stratigraphic architecture depends also on the availability of sediments
1011 and the relation between sedimentation and extension rates. In the Alpine system, sedimentation
1012 during early rifting was controlled by carbonates and thus not controlled by a significant
1013 siliciclastic source. Locally, basins may have been disconnected and a local-derived siliciclastic
1014 source evolved (e.g., *Grès Singuliers* in the example of the Mont Blanc system; Fig. 6a). During
1015 hyperextension, gravitational processes resulted in the deposition of breccias, debris flows and
1016 turbidites. In the case of the Adriatic margin, distal parts were not fed from the continent, and
1017 pelagic and hemipelagic sedimentation, together with reworking of exhumed mantle and
1018 magma emplacement, became the dominant depositional processes. It is important to mention
1019 that the Alpine Tethys example is sediment starved and underfilled. The fill of a humid clastic
1020 run-off dominated basin could look very different as discussed in Part 2 by Chenin et al. (this
1021 volume).

1022 From a structural point of view, two main ways of accommodation creation can be envisaged.
1023 Either by listric, concave-upward normal faults or by concave-downward
1024 extraction/detachment faults (Wilson et al., 2001; Mohn et al., 2012; Petri et al., 2019). While
1025 the first fault type creates fault-bounded basins, the latter fault type results in the creation of
1026 new real estate. In this case, basins become both deeper and wider with increasing extension,
1027 with syn-tectonic sediments directly overlying new real estate (Wilson et al., 2001; Gillard et
1028 al., 2015). It is also important to determine how faults are linked to local flexure and regional
1029 isostasy, which define not only the morphology of top basement, but also the relative timing
1030 between extension and the creation of accommodation. During the stretching phase
1031 accommodation was created mainly by faults, whereas post-rift thermal subsidence was of
1032 minor importance. This is what can be seen in the stretching domain in the proximal margins
1033 of the Alpine Tethys. During the subsequent necking phase, the morphotectonic evolution was
1034 complex and controlled by the formation of a keystone (for a description see Chenin et al.,
1035 2019, 2020), but, on the scale of the rift system, it was symmetric. Examples of this stage are
1036 documented in the Mont Blanc and Briançonnais areas along the European margin, and in the
1037 Cusio–Biellese region on the Adriatic margin (Fig. 6). During the following hyperextension
1038 stage, however, the morphotectonic evolution of the two conjugate systems was very different.
1039 On the lower plate margin (northern Adria), accommodation was controlled proximally
1040 (proximal/inner) by thermal subsidence while distally (distal/outer) it was controlled by the
1041 formation of new real estate between breakaway blocks and extensional allochthons (e.g., Epin
1042 & Manatschal, 2018) (Fig. 7). In contrast, the upper plate showed formation of mega-fault
1043 scarps, which were linked to the formation of prominent and long-lasting mega-breccias and
1044 gravitational systems that faced oceanward a domain of new real estate (see the 2 settings of
1045 type-2 basins in Fig. 5 of Masini et al., 2013). As a consequence, these breccias interfinger with
1046 deep marine sediments at their tips (see Fig. 9 in Ribes et al., 2019b). Some of the breccias may
1047 also have been deposited over exhumation faults and were moved away and were disconnected
1048 from their source on the conjugate margin (see Fig. 8 in Epin et al., 2019). Examples are the

1049 Bernina-Err systems or the lower plate and the Falknis-Tasna for the upper plate setting (Ribes
1050 et al., 2019b) (Fig. 7c). During the formation of the proto-oceanic domain, the system returned
1051 to a more symmetric state and detachment faults showed an interplay between exhumation and
1052 high-angle faulting (Manatschal et al., 2011). This deformation phase, which is observed in the
1053 Platta nappe (Epin et al., 2019), is reminiscent of that observed at slow spreading mid-ocean
1054 ridges (Sauter et al., 2013; Cannat et al., 2019).

1055 *Syn-tectonic fluids and their link to rift evolution*

1056 Little attention has been paid so far to fluids and their link to the rift evolution and related syn-
1057 rift sediments. Pinto *et al.* (2015) and Incerpi *et al.* (2017, 2020) showed that the nature of fluids
1058 was intimately linked to hydrothermal activity during Alpine Tethys rifting. Incerpi *et al.* (2020)
1059 showed that the fluid signature changed from the necking to the hyperextension phase. During
1060 the necking stage, marine-derived fluids interacted with crustal rocks resulting in Si-rich fluids.
1061 Pinto et al. (2015) showed that during the hyperextension phase, marine-derived fluids
1062 circulated along faults down into the exhuming mantle and were channelled back to the seafloor
1063 along detachment faults, forming kilometre-scale hydrothermal cells. These fluids interacted
1064 with the serpentinizing mantle and transported mantle-derived V, Cr, Ni along faults back to
1065 the seafloor. This is well-documented by enrichment of fault rocks and the overlying syn-
1066 tectonic sediments in these mantle-derived elements (Pinto et al., 2015). Coupling the fluid
1067 history with the diagenetic evolution of the syn-rift sediments, as proposed by Incerpi et al.
1068 (2020), may not only enable us to define the depositional setting and the rift domain in which
1069 a sediment has been deposited, but also to use new techniques, such as U-Pb on cements to date
1070 the age of syn-tectonic sequences. Moreover, potential links between the widespread
1071 development of siliceous sediments and organisms, i.e., radiolarite, and tectonic exhumation
1072 and related Si-rich fluids may exist (Pinto et al., 2017).

1073 **ALONG STRIKE VARIABILITY OF THE ALPINE TETHYS RIFT** 1074 **SYSTEM**

1075 Our description of the Alpine Tethys rift system and of its evolution is mainly based on a few
1076 building blocks (BBs), most of which are located in the central Piemonte segment of the Alpine
1077 Tethys (Figs. 1a and 4). However, this 2D view underscores the non-cylindricity and 3D
1078 complexity of the Alpine Tethys, which can be regarded from different scale perspectives.

1079 From a large-scale perspective, the Alpine Tethys is only one out of at least three rift systems,
1080 referred to as *Meliata/Vardar/E-Mediterranean*, *Alpine Tethys*, and *Iberia/Pyrenees/Bay of*
1081 *Biscay* (Fig. 1b). The spatial overlap of these multistage rift systems makes it difficult not only
1082 to determine the timing of rift onset in individual areas, in particular where such systems
1083 overlap, but also to unravel the subsidence history, since the post-rift of one stage can
1084 correspond to the pre-rift of the next stage. An example is, for instance, the thick Triassic
1085 dolostones in the Adria and Briançonnais domains, which are syn- to post-rift with respect to
1086 the Meliata/Vardar, but pre-rift with respect to the Alpine Tethys (violet sediments in Fig. 10e).
1087 Other examples are the Cretaceous extensional systems that are linked to the Pyrenean phase
1088 of rifting, which overlap Jurassic rift domains in the European margin (Tavani et al., 2018). At
1089 present, the partitioning of extension between these rift systems remains little constrained since
1090 no undisputed data exist on the width, rates, or the detailed kinematic movements of any of

1091 these interacting systems. Our preferred view is that the Alpine Tethys rifting initiated during
1092 the latest Triassic (200 ± 5 Ma) and stopped in the Late Jurassic time as a failed, approximately
1093 300 to 400 km-wide, proto-oceanic domain (Li et al. 2013).

1094 At the scale of the Alpine Tethys, three segments can be distinguished, the *Ligurian*, *Piemonte*
1095 and *Valais* basins (Figs. 1a and 4). Thermochronological and stratigraphic data suggest that
1096 these basins may have started to become well-defined structural entities during the
1097 Sinemurian/Pliensbachian (Fig. 4b), and may have merged into a unique, proto-oceanic or
1098 oceanic domain, which is referred to as the Alpine Tethys, during the Callovian/Bathonian
1099 (Baumgartner, 2013) (Fig. 4a). However, many questions remain open, especially about the
1100 southern Ligurian domain. To date, it remains unclear whether this basin had a Triassic
1101 precursor basin and if it was linked to the eastern Mediterranean, as suggested by its thick and
1102 locally deep Triassic sequences (Speranza et al., 2012). The Alpine Tethys rift system may have
1103 had overstepping accommodation zones, similar to what has been proposed for the Cretaceous
1104 basins in the Pyrenean domain (Lescoutre & Manatschal, 2020). The formation of continental
1105 ribbons such as the Briançonnais, separating two V-shaped hyperextended domains that were
1106 set up as overstepping accommodation zones and merged during breakup, may be a reasonable
1107 explanation. This hypothesis remains yet to be confirmed by field data. However, it is
1108 interesting to note that in the Biscay and Pyrenean domains, rift segment centres of
1109 hyperextended basins are often completely reactivated (subducted). In contrast at rift segment
1110 boundaries rift structures remain preserved in the mountain belt. This has been explained by
1111 thrusts forming shortcuts to link one segment to another (Lescoutre & Manatschal, 2020;
1112 Manatschal et al., 2021). This may explain why the best-preserved rift structures occur on both
1113 sides of the Peri-Adriatic system (e.g., Insubric line that is the boundary between an upper and
1114 a lower plate; Decarlis et al., 2017) or are linked to the Briançonnais block. In any case,
1115 whatever the actual architecture of the Alpine Tethys looked like, it was clearly not cylindrical.
1116 The relationships between the Ligurian and Piemonte segments of the rift system appear, in
1117 contrast, simpler and seem to coincide with the paleo-Insubric transfer system.

1118 The complex paleogeography of the former Alpine Tethys rift system is not very different from
1119 that observed at many Atlantic margins. The paleogeography of the Alpine Tethys rift system
1120 has important implications on how and where sediments were transported into the deep margins
1121 (e.g., Ribes et al., 2019b). The segmented paleogeography of the Alpine Tethys can partly
1122 explain why the Alpine terminology is so complex and the paleogeographic domains cannot be
1123 correlated along the Alps in a simple way. Thus, most of the controversies based on correlations
1124 between Alpine units and domains may be solved, or at least better defined, when the complex
1125 pre-Alpine paleogeography and segmentation are better understood.

1126 **THE SYN-RIFT STRATIGRAPHIC ARCHITECTURE OF THE ALPINE**
1127 **TETHYS: AN OUTLOOK**

1128 The Alps have been the origin of many ideas and concepts presently used not only in orogenic
1129 belts, but also at rifted margins (De Graciansky et al., 2011). Long before rifted margins were
1130 seismically imaged, Alpine geologists proposed that the sediments were deposited in large
1131 basins, first called geosynclines, and later rift basins. Research over the past decades show that
1132 the Alps are not so much influenced by the subduction of an oceanic domain, but more by the
1133 reactivation of former rifted margins. Research on rifted margins has mainly been triggered in
1134 the last years by the energy industry and the related progress in reflection seismic imaging and
1135 numerical modelling. However, the Alps have played a critical role in the latest development
1136 of understanding distal rifted margins with the discovery and description of the hereby
1137 described “building blocks” / BBs, their integration in a margin template and the access of a
1138 data set and observations that are not accessible at present-day rifted margins. This enabled us
1139 to develop a model to describe the tectono-stratigraphic evolution of a magma-poor rifted
1140 margin. A prerequisite for such a model is to integrate time into a spatial reconstruction. This
1141 can be done by relying on two types of data. On one hand, petrological and thermochronological
1142 data provide insight into the PTt path of basement rocks. On the other hand, sedimentary
1143 deposits act as a tape recorder of the evolving deformation and depositional environments.
1144 Whenever timelines can be identified throughout the margin, they give insight into the
1145 migration of deformation through time along the margin (e.g., Ribes et al., 2019a). In addition,
1146 with the development of the BB approach it was possible to build generic sections across
1147 margins. As each BB represents a “frozen” structural template with specific structural,
1148 stratigraphic, thermochronological and petrological characteristics, the comparison between the
1149 different BB characteristics provides insights into the temporal evolution of the entire rift
1150 system. This methodology enabled Masini et al. (2013) and Ribes et al. (2019a) to demonstrate
1151 the migration of rift activity from the future proximal margins towards the future distal margins,
1152 and to point out the onset of rifting in the Alpine Tethys domain, the crucial moment of necking,
1153 and the timing of first magma-production in the exhumed domain. Moreover, it allowed them
1154 to identify different rift phases, and to define rift domains and the specific time periods during
1155 which they formed.

1156 However, the study of rifted margins worldwide, in particular of their distal parts, is notoriously
1157 limited by the lack data. While many high-resolution 3D seismic blocks of distal margins
1158 became recently available to researchers, and although numerical modelling is able to reproduce
1159 some of the key rift structures in 2D and/or 3D, the access to samples from these domains
1160 remains the biggest issue. Deep-sea drilling is expensive and remains exceptional; where
1161 available, it is generally restricted to structural highs, rarely transecting deep depocenters and/or
1162 penetrating the underlying basement. Therefore, a major asset for research on rifted margins in
1163 the Alps is the possibility to put specific outcrops into the framework of a present-day rifted
1164 margin, to further calibrate the new models and to make predictions of how the new concepts
1165 can be used to make projections from well calibrated proximal to undrilled distal domains.
1166 However, there are also limitations to the extent the Alpine Tethys can be used to compare with
1167 other margins. Future research will need to better define the 3D spatial framework and temporal
1168 development of rifting processes. This includes the semi-quantitative analysis of vertical and
1169 horizontal movements during rifting, the characterization of the successive deformation events,
1170 and the recognition of related depositional systems. Part II of this review (Chenin et al., this
1171 volume) will build on observations and concept derived from the Alps to propose a more
1172 generic model that will then be tested/discussed using global examples of present-day rifted
1173 margins.

1174 **ACKNOWLEDGMENTS**

1175 The authors are grateful to C.A.L. Jackson, I. Sharp, A. Pfiffner and S. Tavani for
1176 thorough and very constructive reviews that helped improving the manuscript. We also
1177 thank Editor K. Gallagher for handling both the present manuscript and its companion.
1178 Moreover, we would like to thank all PhD students, Post Docs and colleagues, too
1179 numerous to name all, for the discussions and debates through the last 25 years on
1180 the Alps and its pre-Alpine evolution.

1181

1182 Author contributions:

1183 Gianreto Manatschal: Writing – original draft, Conceptualization, Investigation,
1184 Funding acquisition

1185 Pauline Chenin: Writing – review & editing, Conceptualization, Investigation

1186 Jean-François Ghienne: Writing – review & editing, Conceptualization, Investigation

1187 Charlotte Ribes: Writing – review & editing, Conceptualization, Investigation

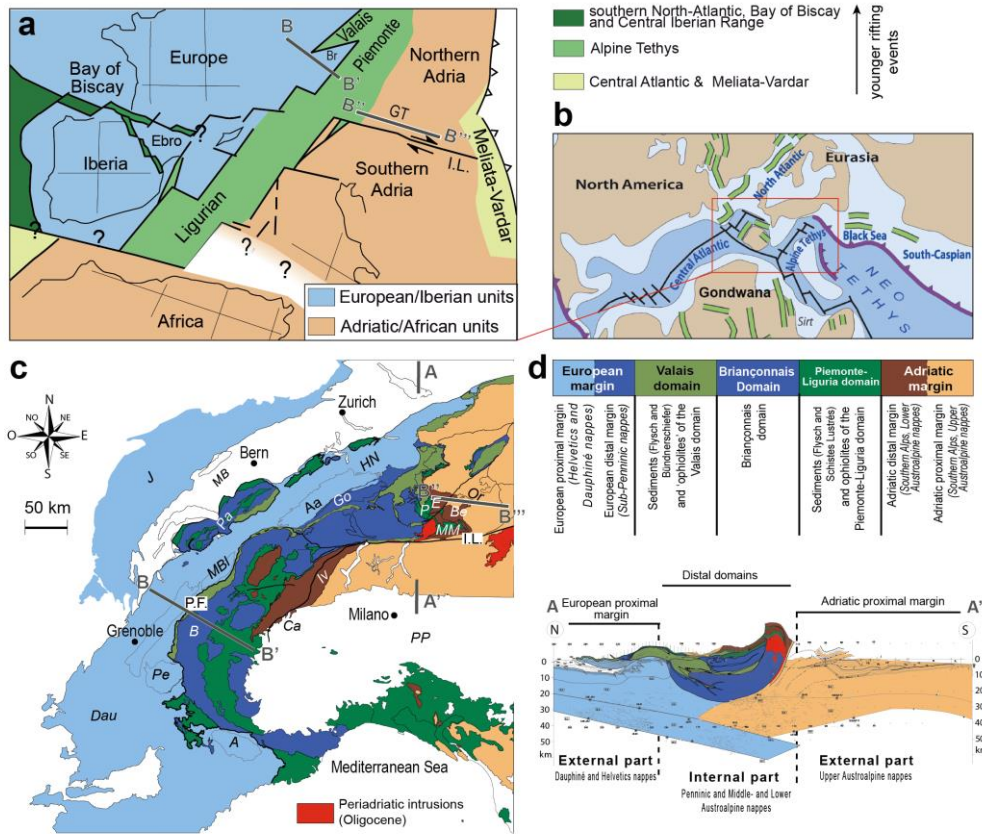
1188 Emmanuel Masini: Writing – review & editing, Conceptualization, Investigation

1189

1190

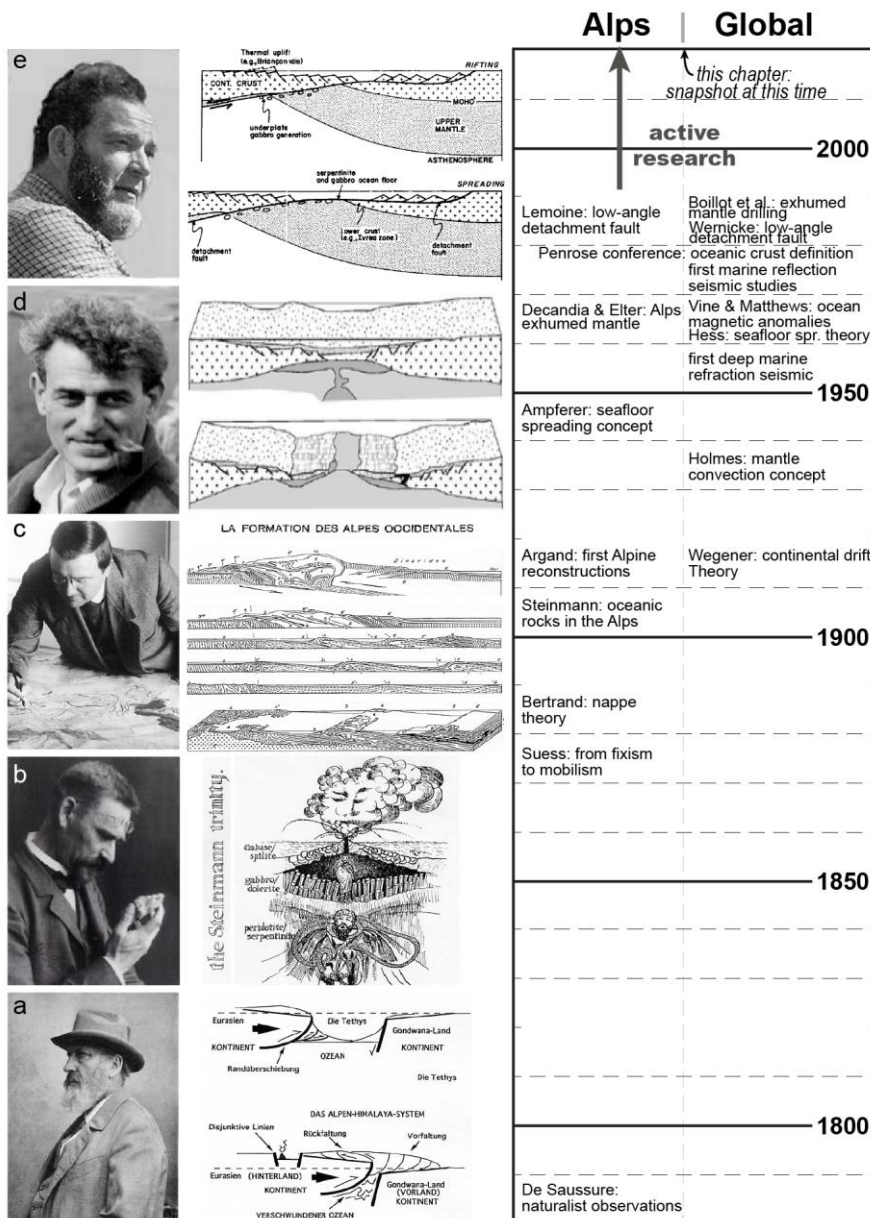
1191 Data Availability Statement:

1192 Data sharing is not applicable to this article as no new data were created or analyzed
1193 in this study.



1195

1196 **Fig. 1.** (a) Schematic paleogeographic map of the Tethys – Atlantic domain during Early
 1197 Cretaceous showing three main rift-systems (Meliata-Vardar; Alpine Tethys (Liguria,
 1198 Piemonte, Valais); and southern North Atlantic with the Bay of Biscay-Pyrenean and
 1199 Central Iberian Range) and surrounding major plates (Africa and Europe) and
 1200 microplates (Iberia, Ebro, Southern Adria and Northern Adria) (modified after
 1201 Manatschal and Müntener, 2009). (b) Paleogeographic map of the western Tethys and
 1202 Central and North Atlantic system during Early Cretaceous (modified after Frizon de
 1203 Lamotte et al., 2015). The red box shows the outline of the area shown in Fig. 1a. (c)
 1204 Tectonic map of the Alps in Western Europe showing the distribution of the main
 1205 paleogeographic rift domains of the Alpine Tethys in the Alpine orogen (modified
 1206 after Schmid et al., 2004). (d) Interpretation of the NFP 20 seismic section across the
 1207 Central Alps showing the position of the main paleogeographic rift domains in the
 1208 Alpine section (modified after Schmid et al., 1996). For location of the section A-A'
 1209 see (c). The B–B' and the B''–B''' transects correspond to sections across the former
 1210 European margin and the Grischun transect (GT) across the northern Adria margin that
 1211 will be presented in Figs. 3, 9 and 10. Note that these two transects are not conjugate
 1212 margins but are interpreted to belong both to the Piemonte rift segment. Abbreviations
 1213 used in Fig. 1: A: Argentera Massif, Aa: Aar Massif, B: Briançonnais Nappes, Be:
 1214 Bernina Ca: Canavese Nappe, Dau: Dauphiné Nappes, E: Err Nappe, Go: Gotthard
 1215 Massif, HN: Helvetic Nappes, Iv: Ivrea, J: Jura, MB: Molasse Basin, MBI: Mont
 1216 Blanc Massif, MM: Malenco-Margna Nappes, Or: Ortler Nappe, P: Platta Nappe, Pa:
 1217 Prealps, Pe: Pelvoux Massif, PP: Po Plain.

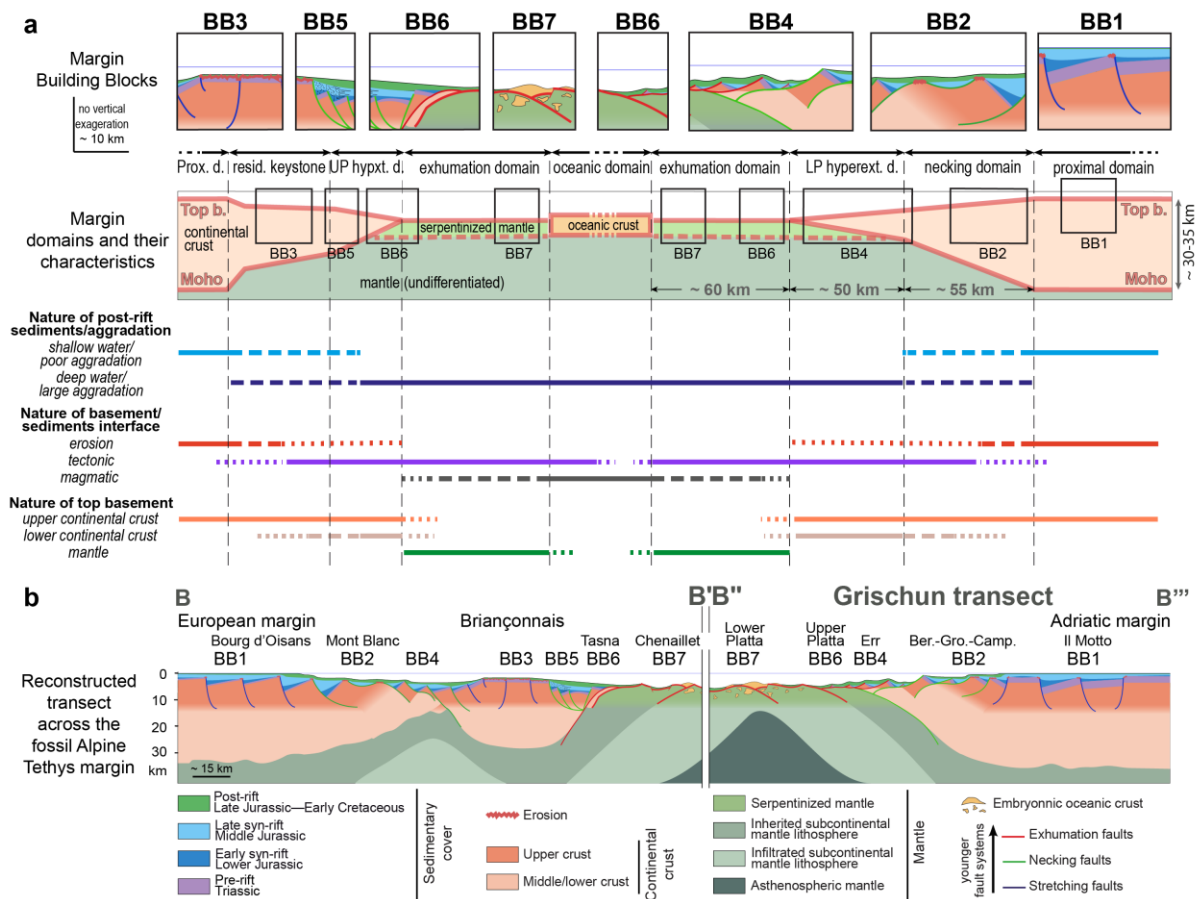


1218

1219

Fig. 2: Evolution of concepts and important players of the “Alpine Tethys”: (a) Eduard Suess was among the first to recognize the existence of former basins in the Alpine domain, which he named Tethys; figure from Suess (1875). (b) Gustave Steinmann was among the first to recognize and map the serpentized peridotite–“diabase”–radiolarite association (the Steinmann trinity) throughout the Alps and to interpret it as a remnant of a fossil deep ocean floor; figure from Coleman (1977). (c) Emile Argand was among the first to propose detailed tectonic and paleogeographic restorations by applying a mobilistic view to the Alpine system; figure from Argand (1916). (d) Piero Elter was the first who suggested mantle exhumation and therefore the magma-poor nature of the Alpine Tethys; figure from Decandia and Elter (1972). (e) Marcel Lemoine was at the forefront of the present-day interpretation of the Alpine Tethys as a magma-poor, polyphase rifted margin; figure from Lemoine et al. (1987).

1230



1231

1232

1233

1234

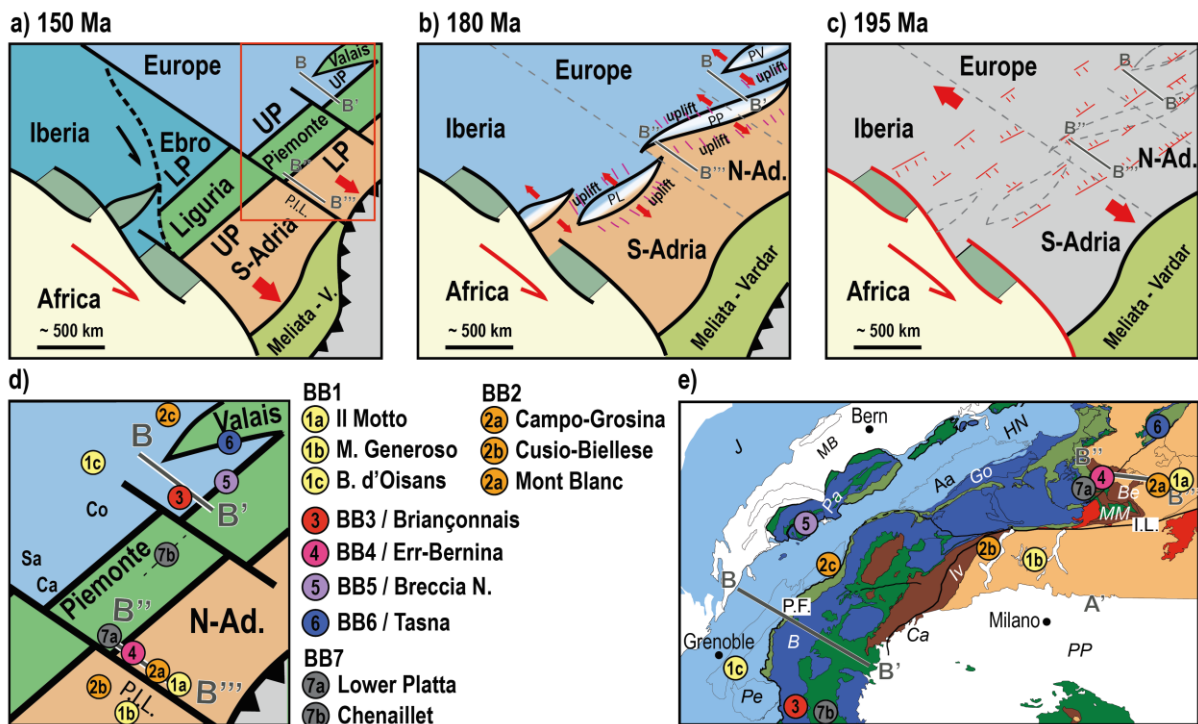
1235

1236

1237

1238

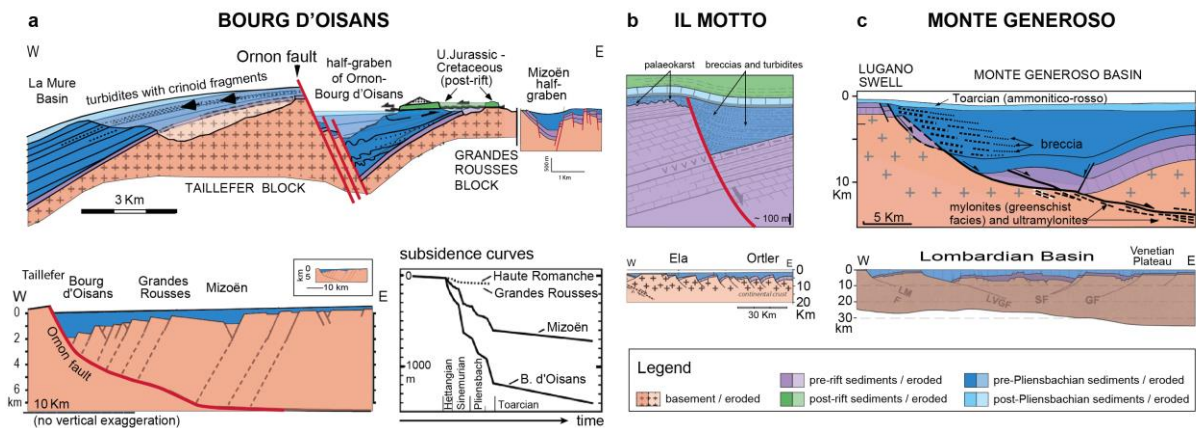
Fig. 3: The Building Block (BB) concept applied to the Alpine Tethys margins: (a) Schematic section across a conjugate magma-poor rifted margin pair and location of the building blocks (BB) (see text for details). The nature of top basement, post-rift sediments, and of their interface vary across the margin and is diagnostic to define rift domains (see Tugend et al., 2014). b) Synthetic reconstruction of a composite transect across the Alpine Tethys rift system (see Fig. 1 for location of B–B' and B''–B''' transects) and location of BBs and projected position of type localities.



1239

1240
 1241
 1242
 1243
 1244
 1245
 1246
 1247
 1248
 1249
 1250

Fig. 4: Schematic maps showing the paleogeographic evolution of the Alpine Tethys at: (a) Late Jurassic (150 Ma; assumed end of rifting/spreading in the Alpine Tethys); (b) Late Pliensbachian (180 Ma; end of necking phase); (c) Early Jurassic (195 Ma; stretching phase). Interpretation based on Decarlis et al., 2018). The interpretation assumes that individual basins formed as segmented en-echelon rift segments separated by accommodation/transfer zones. (d) Zoom on (a) showing the locations of the BBs described in this study at Late Jurassic time, and (e) location of the BBs on the present-day structural map shown in Fig. 1c. Abbreviations: P.I.L.: Paleo Insubric Line; PL: Proto Liguria basin; PP: Proto Piemonte basin; PV: Proto Valais basin; LP: Lower Plate; UP: Upper Plate. Transects B-B' and B''-B''' (for position see also Fig. 1).



1252

1253

1254

1255

1256

1257

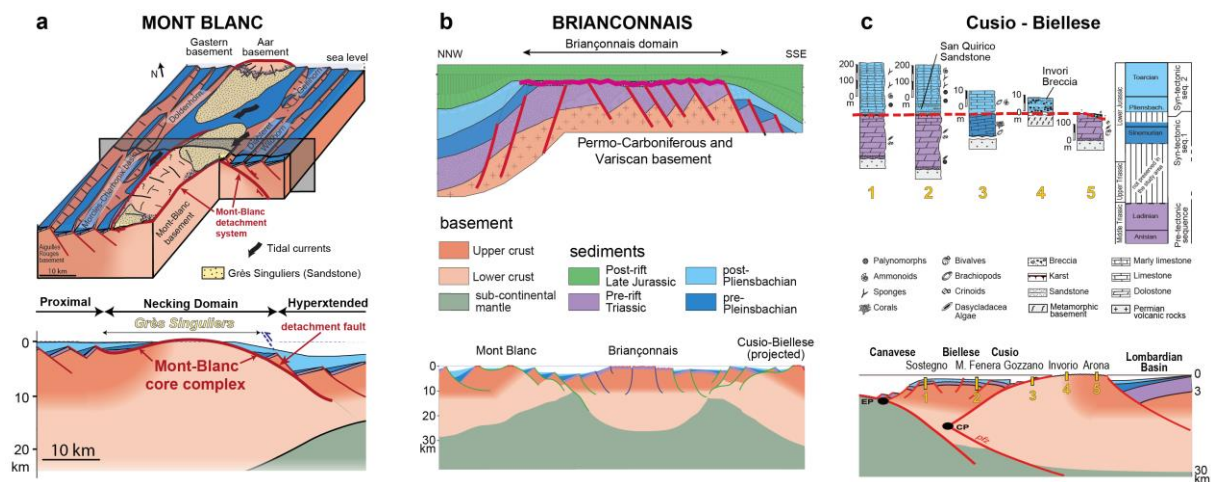
1258

1259

1260

1261

Fig. 5: Examples of BB1 exposed in the Alps documenting the stretching stage observed in the proximal Alpine Tethys margins: (a) the Bourg d’Oisans Basin in the proximal European margin (modified after Chevalier, 2002 and De Graciansky et al., 2012); (b) Il Motto Basin in the Upper Austroalpine Ortler Nappe near Livigno in northern Italy belonging to the former northern Adria proximal margin (modified after Eberli, 1988 and De Graciansky et al., 2012); and (c) the Monte Generoso Basin in the Southern Alps belonging to the former southern Adria margin (modified after Bertotti et al., 1993 and De Graciansky et al., 2012).



1262

1263

1264

1265

1266

1267

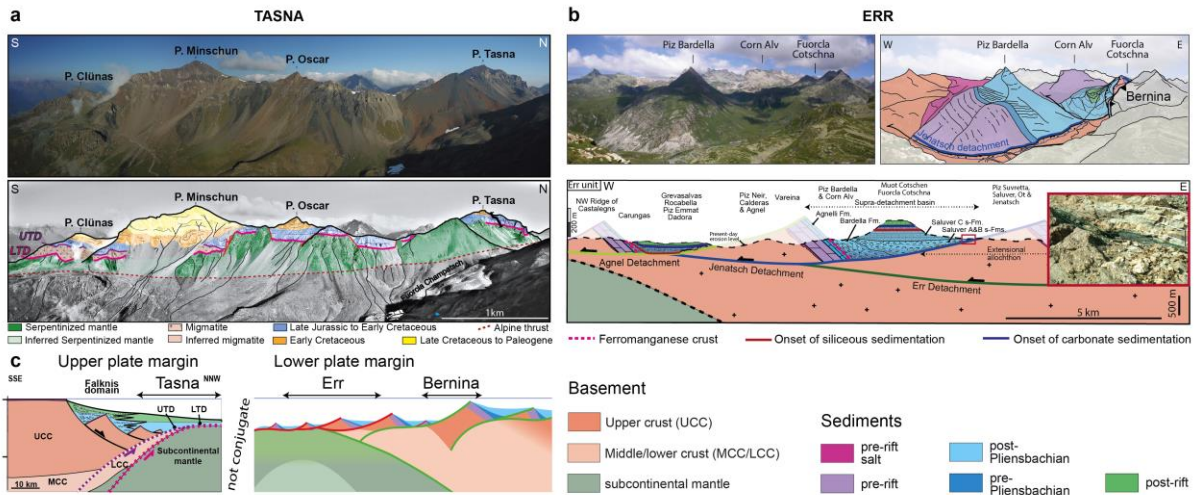
1268

1269

1270

1271

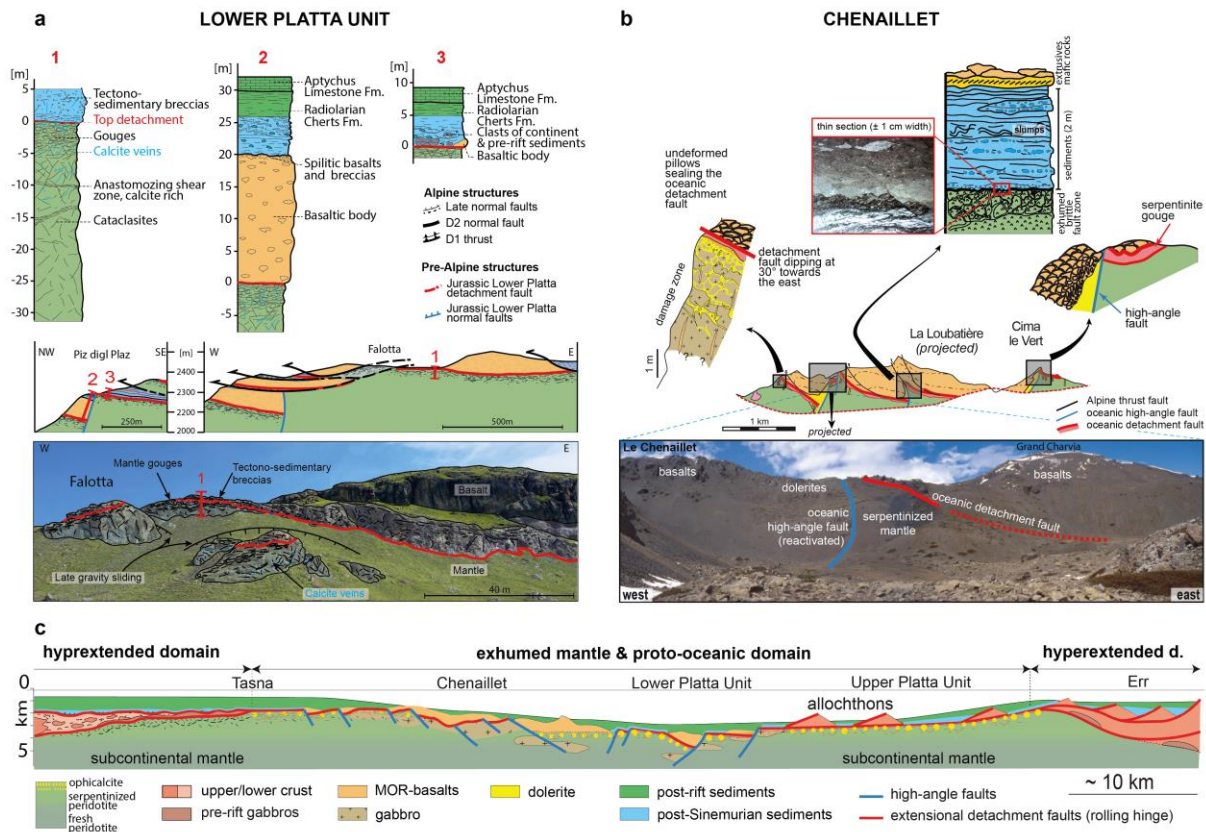
Fig. 6: Examples of BB2 and BB3 exposed in the Alps documenting the necking stage observed at the transition between the proximal and distal Alpine Tethys margins and the future distal part before onset of hyperextension: (a) Mont Blanc core complex representing a remnant of the European necking domain (modified after Ribes et al., 2020a); (b) the Briançonnais domain representing the future distal European margin characterized by a major necking unconformity (modified after De Graciansky et al., 2012); (c) The Cusio – Biellese domain showing the stratigraphic record of the southern Adria necking domain (modified after Beltrando et al., 2015 and Decarlis et al., 2018).



1272

1273 **Fig. 7:** Examples of BB4, BB5 and BB6 exposed in the Alps documenting the hyperextension
 1274 and early mantle exhumation stage observed in the distal Alpine Tethys margins: (a)
 1275 Tasna exposed in the Tasna Nappe in the Engadin Window north of Scuol (SE
 1276 Switzerland) and representing the most distal European/Briançonnais margin
 1277 (modified after Ribes et al., 2020b) (UTD: Upper Tasna Detachment; LTD: Lower
 1278 Tasna Detachment); (b) Err exposed in the Lower Austroalpine Err Nappe in SE
 1279 Switzerland showing the Bardella extensional allochthon at the Julier Pass; photograph
 1280 on the lower right corner shows the onlap of syn-tectonic sandstones onlapping onto
 1281 the detachment surface indicated by the black colored fault gouges; modified after
 1282 Epin & Manatschal (2018) and Ribes et al. (2019a).

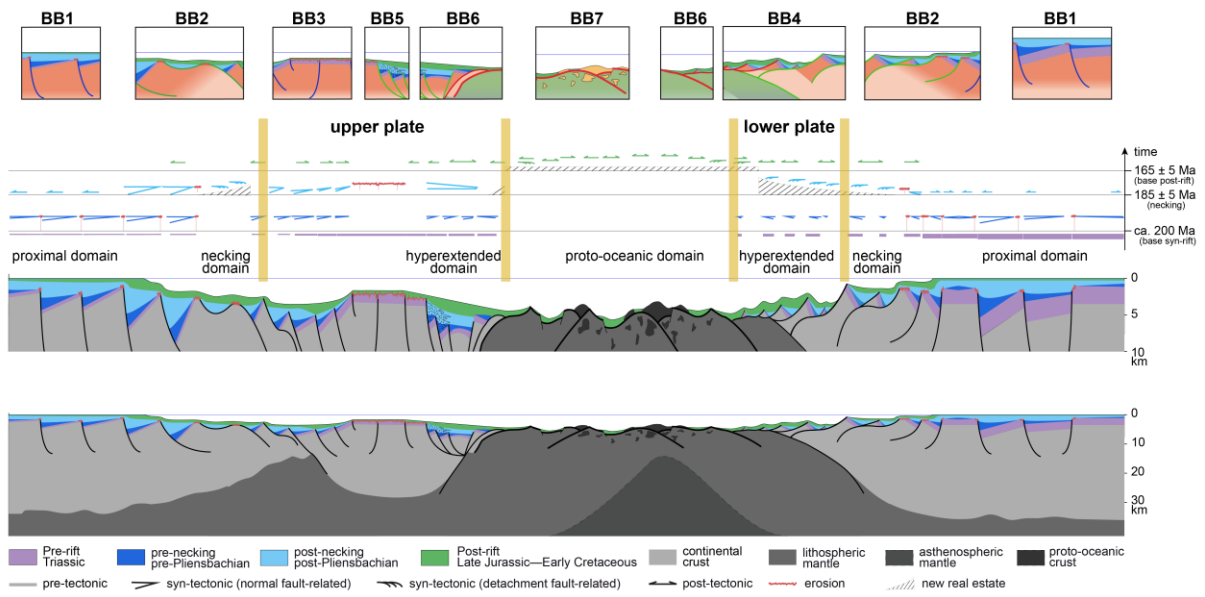
1283



1284

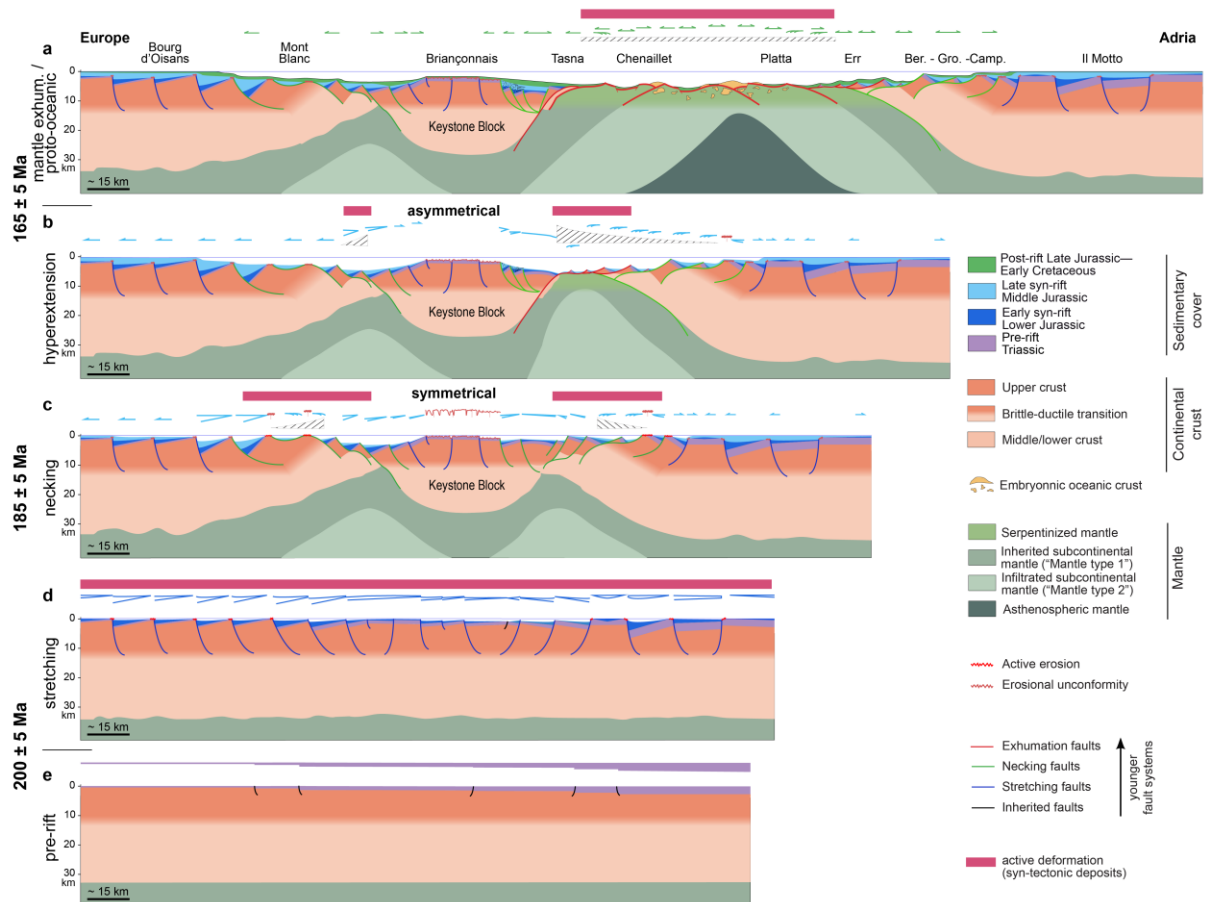
1285
1286
1287
1288
1289
1290
1291
1292

Fig. 8: Examples of BB7 exposed in the Alps documenting early seafloor spreading (proto-oceanic crust) of the Alpine Tethys: (a) the Lower Platta Unit exposed in the Val Surses in SE Switzerland (modified after Epin et al., 2019); (b) Chanaillet Ophiolite exposed near Briançon along the French/Italian border in the Western Alps (modified after Manatschal et al., 2011); (c) section across the Ocean Continent Transition of the Alpine Tethys showing the transition from hyperextended crust to exhumed mantle and then to proto-oceanic crust (modified after Manatschal & Müntener, 2009). Section (c) shows localities in (a) and (b).



1295
 1296
 1297
 1298

Fig. 9: Section across the Alpine Tethys corresponding to transects introduced in Fig. 3 (for location see Figs. 1 and 4). The section highlights the stratigraphic architecture of the Alpine Tethys margins across the central Piemonte segment and document the syn-tectonic evolution in the overlying Wheeler diagram (for details see text).



1299

1300 **Fig. 10:** Main phases of the Alpine Tethys rift evolution: (a) mantle exhumation phase and
 1301 embryonic seafloor spreading (formation of proto-oceanic crust); (b) hyperextension
 1302 phase; (c) necking phase; (d) stretching phase; (e) initial stage. See text for a detailed
 1303 description of the evolution.

1304

1305

	BB1	BB2	BB3	BB4	BB5	BB6	BB7
rift domain	proximal (stretching)	necking	necking (residual keystone)	hyperextended (lower plate)	hyperextended (upper plate)	exhumed	proto-oceanic
type basement	upper continental crust	upper/middle continental crust	upper continental crust	upper/lower continental crust	upper/lower continental crust	exhumed mantle	exhumed mantle/magma
fault-types	high-angle faults	high/low-angle faults	high-angle faults	high/low-angle faults	high/low-angle faults	high/low-angle faults	high/low-angle faults
bathymetry (during formation)	shallow/subareal	shallow/subareal	shallow/subareal	deep/subsiding	deep/subsiding	deep/subsiding	deep/subsiding
type locality (see Fig. 4d & e)	Il Motto / Generoso / Bourg d'Oisans)	Campo-Grosina/ Mont Blanc/Cusio-Biellese)	Fond Froid – Lac de l'Ascension (Briançonnais)	Err & Bernina	Breccia Nappe	Tasna OCT	Lower Platta / Chenaillet
key reference	Eberli 1988 Ribes et al. 2019a	Mohn et al. 2012 Ribes et al. 2020a	Claudel & Dumont, 1999	Masini et al., 2012 Epin & Manatschal, 2018	Escher et al. 1993 Steffen et al. 1993	Ribes et al. 2020b	Epin et al. 2019, Manatschal et al. 2011

1306

1307 Table 1: Overview of Building Blocks defined for the Alpine Tethys

1308

References:

- 1309 Amann, M., Ulrich, M., Manatschal, G., Pelt, E., Epin, M.E., Autin, J., Sauter, D., 2020. Geochemical
1310 characteristics of basalts related to incipient oceanization: The example from the Alpine-Tethys
1311 OCTs. *Terra Nov.* 32, 75–88. <https://doi.org/10.1111/ter.12438>
- 1312 Angrand, P., Mouthereau, F., Masini, E., Asti, R., 2020. A reconstruction of Iberia accounting for
1313 Western Tethys-North Atlantic kinematics since the late-Permian-Triassic. *Solid Earth* 11, 1313–
1314 1332. <https://doi.org/10.5194/se-11-1313-2020>
- 1315 Argand, E., 1916. Sur l'arc des Alpes occidentales. Bridel, G.
- 1316 Badoux, H., & Mercanton, C. H. (1962). Essai sur l'évolution tectonique des Préalpes médianes du
1317 Chablais. Birkhäuser.
- 1318 Barboza, S.A., Bergantz, G.W., Brown, M., 1999. Regional granulite facies metamorphism in the Ivrea
1319 zone: Is the Mafic Complex the smoking gun or a red herring? *Geology* 27, 447–450.
1320 [https://doi.org/10.1130/0091-7613\(1999\)027<0447:rgfmit>2.3.co;2](https://doi.org/10.1130/0091-7613(1999)027<0447:rgfmit>2.3.co;2)
- 1321 Barfety, J. C. (1985). Le Jurassique dauphinois entre Durance et Rhône: étude stratigraphique et
1322 géodynamique; évolution d'une portion de la marge nord téthysienne (Alpes occidentales
1323 françaises) (Doctoral dissertation, Université Scientifique et Médicale de Grenoble).
- 1324 Barnett-Moore, N., Hosseinpour, M., Maus, S., 2016. Assessing discrepancies between previous plate
1325 kinematic models of Mesozoic Iberia and their constraints. *Tectonics* 35, 1843–1862.
1326 <https://doi.org/10.1002/2015TC004019>
- 1327 Baumgartner, P.O., 2013. Mesozoic radiolarites - accumulation as a function of sea surface fertility on
1328 Tethyan margins and in ocean basins. *Sedimentology* 60, 292–318.
1329 <https://doi.org/10.1111/sed.12022>
- 1330 Beltrando, M., Compagnoni, R., Ferrando, S., Mohn, G., Frasca, G., Odasso, N., ... & Beltrando, M.
1331 (2014). Crustal thinning and mantle exhumation in the Levone area (Southern Canavese Zone,
1332 Western Alps). *A Field Guide Across the Margins of Alpine Tethys*, *Journal of the Virtual*
1333 *Explorer, Electronic Edition*, 48.
- 1334 Beltrando, M., Stockli, D.F., Decarlis, A., Manatschal, G., 2015. A crustal-scale view at rift localization
1335 along the fossil Adriatic margin of the Alpine Tethys preserved in NW Italy. *Tectonics* 34, 1927–
1336 1951. <https://doi.org/10.1002/2015TC003973>
- 1337 Bernoulli, D., 1964. Zur Geologie des Monte Generoso (Lombardische Alpen): ein Beitrag zur
1338 Kenntnis der südalpinen Sedimente.
- 1339 Berra, F., Galli, M. T., Reghellin, F., Torricelli, S., & Fantoni, R. (2009). Stratigraphic evolution of the
1340 Triassic–Jurassic succession in the Western Southern Alps (Italy): the record of the two-stage

- 1341 rifting on the distal passive margin of Adria. *Basin Research*, 21(3), 335-353.
- 1342 Bertotti, G., 1991. Early Mesozoic extension and Alpine shortening in the western Southern Alps: The
1343 geology of the area between Lugano and Menaggio (Lombardy, Northern Italy). *Mem. Soc. Geol.*
1344 Padova 43, 17–123.
- 1345 Bertotti, G., Picotti, V., Bernoulli, D., & Castellarin, A. (1993). From rifting to drifting: tectonic evolution
1346 of the South-Alpine upper crust from the Triassic to the Early Cretaceous. *Sedimentary Geology*,
1347 86(1-2), 53-76.
- 1348 Bertrand, M., 1884. Rapports de structure des Alpes de Glaris et du bassin houiller du Nord. *Bull. la*
1349 *Société Géologique Fr.* 3, 318–330.
- 1350 Bill, M., O'Dogherty, L., Guex, J., Baumgartner, P. O., & Masson, H. (2001). Radiolarite ages in
1351 Alpine-Mediterranean ophiolites: Constraints on the oceanic spreading and the Tethys-Atlantic
1352 connection. *GSA Bulletin*, 113(1), 129-143.
- 1353 Boillot, G., Recq, M., Winterer, E.L., Meyer, A.W., Applegate, J., Baltuck, M., Bergen, J.A., Comas,
1354 M.C., Davies, T.A., Dunham, K., Evans, C.A., Girardeau, J., Goldberg, G., Haggerty, J., Jansa,
1355 L.F., Johnson, J.A., Kasahara, J., Loreau, J.P., Luna-Sierra, E., Moullade, M., Ogg, J., Sarti, M.,
1356 Thurow, J., Williamson, M., 1987. Tectonic denudation of the upper mantle along passive
1357 margins: a model based on drilling results (ODP leg 103, western Galicia margin, Spain).
1358 *Tectonophysics* 132, 335–342. [https://doi.org/10.1016/0040-1951\(87\)90352-0](https://doi.org/10.1016/0040-1951(87)90352-0)
- 1359 Bonin, B., Azzouni-Sekkal, A., Bussy, F., Ferrag, S., 1998. Alkali-calcic and alkaline post-orogenic
1360 (PO) granite magmatism: Petrologic constraints and geodynamic settings. *Lithos* 45, 45–70.
1361 [https://doi.org/10.1016/S0024-4937\(98\)00025-5](https://doi.org/10.1016/S0024-4937(98)00025-5)
- 1362 Cannat, M., Sauter, D., Lavier, L., Bickert, M., Momoh, E., Leroy, S., 2019. On spreading modes and
1363 magma supply at slow and ultraslow mid-ocean ridges. *Earth Planet. Sci. Lett.* 519, 223–233.
1364 <https://doi.org/10.1016/j.epsl.2019.05.012>
- 1365 Chenin, P., Manatschal, G., Decarlis, A., Schmalholz, S.M., Duretz, T., Beltrando, M., 2019. Emersion
1366 of distal domains in advanced stages of continental rifting explained by asynchronous crust and
1367 mantle necking. *Geochemistry, Geophys. Geosystems* 2019GC008357.
1368 <https://doi.org/10.1029/2019GC008357>
- 1369 Chenin, P., Manatschal, G., Picazo, S., Müntener, O., Karner, G.D., Johnson, C., Ulrich, M., 2017.
1370 Influence of the architecture of magma-poor hyperextended rifted margins on orogens produced
1371 by the closure of narrow versus wide oceans. *Geosphere* 13, 1–18.
1372 <https://doi.org/10.1130/GES01363.1>
- 1373 Chenin, P., Picazo, S., Jammes, S., Manatschal, G., Müntener, O., Karner, G., 2018a. Potential role of
1374 lithospheric mantle composition in the Wilson cycle: a North Atlantic perspective, in: WILSON,
1375 R.W., HOUSEMAN, G.A., MCCAFFREY, K.J.W., DORÉ, A.G., BUITER, S.J.H. (Eds.), *Fifty*
1376 *Years of the Wilson Cycle Concept in Plate Tectonics*. Geological Society, London, Special
1377 Publications, 470. <https://doi.org/10.1144/SP470.10>

- 1378 Chenin, P., Schmalholz, S.M., Manatschal, G., Duret, T., 2020. Impact of crust–mantle mechanical
1379 coupling on the topographic and thermal evolutions during the necking phase of ‘magma-poor’
1380 and ‘sediment-starved’ rift systems: A numerical modeling study. *Tectonophysics* 228472.
1381 <https://doi.org/10.1016/j.tecto.2020.228472>
- 1382 Chenin, P., Schmalholz, S.M., Manatschal, G., Karner, G.D., 2018b. Necking of the lithosphere: A
1383 reappraisal of basic concepts with thermo-mechanical numerical modeling. *J. Geophys. Res.*
1384 *Solid Earth* 123, 5279–5299. <https://doi.org/10.1029/2017JB014155>
- 1385 Chessex, R.: La géologie de la haute vallée d'Abondance, Haute-Savoie, France. -- *Ecl. Geol. Helv.*,
1386 52, p. 295, 1959.
- 1387 Chevalier, F. (2002). Vitesse et cyclicité de fonctionnement des failles normales de rift: implication sur
1388 le remplissage stratigraphique des bassins et sur les modalités d'extension d'une marge passive
1389 fossile: application au demi-graben liasique de Bourg-d'Oisans (Alpes occidentales, France)
1390 (Doctoral dissertation, Université de Bourgogne).
- 1391 Chevalier, F., Guiraud, M., Garcia, J. P., Dommergues, J. L., Quesne, D., Allemand, P., & Dumont, T.
1392 (2003). Calculating the long-term displacement rates of a normal fault from the high-resolution
1393 stratigraphic record (early Tethyan rifting, French Alps). *Terra Nova*, 15(6), 410-416.
- 1394 Claudel, M.E., Dumont, T., 1999. A record of multistage continental break-up on the Briançonnais
1395 marginal plateau (Western Alps): Early and Middle-Late Jurassic rifting. *Eclogae Geol. Helv.* 92,
1396 45–61.
- 1397 Coleman, R.G., 1977. Ophiolites. Ancient oceanic lithosphere. Springer-Verlag, Berlin, Heidelberg,
1398 New York. Coltat, R., Branquet, Y., Gautier, P., Campos Rodriguez, H., Poujol, M., Pelleter, E., ...
1399 & Boulvais, P. (2019a). Unravelling the root zone of ultramafic-hosted black smokers-like
1400 hydrothermalism from an Alpine analog. *Terra Nova*, 31(6), 549-561.
- 1401 Coltat, R., Boulvais, P., Branquet, Y., Collot, J., Epin, M. E., & Manatschal, G. (2019b). Syntectonic
1402 carbonation during synmagmatic mantle exhumation at an ocean-continent transition. *Geology*,
1403 47(2), 183-186.
- 1404 Coltat, R., Branquet, Y., Gautier, P., Boulvais, P., & Manatschal, G. (2020). The nature of the interface
1405 between basalts and serpentinitized mantle in oceanic domains: Insights from a geological section
1406 in the Alps. *Tectonophysics*, 797, 228646.
- 1407 Conti, P., Manatschal, G., & Pfister, M. (1994). Synrift sedimentation, Jurassic and Alpine tectonics in
1408 the central Ortler nappe (Eastern Alps, Italy). *Eclogae Geologicae Helveticae*, 87(1), 63-90.
- 1409 Costamagna, L. G. (2016). The Middle Jurassic Alpine Tethyan unconformity and the Eastern
1410 Sardinia–Corsica Jurassic high: A sedimentary and regional analysis. *Journal of Iberian Geology*,
1411 42(3), 311–334. Debelmas, J., 1955. Les zones subbriançonnaise et briançonnaise occidentale
1412 entre Vallouise et Guillestre (Hautes-Alpes).
- 1413 Decandia, F.A., Elter, P., 1969. Riflessioni sul problema delle ofioliti nell'Appennino settentrionale
1414 (nota preliminare). *Atti della Soc. Toscana di Sci. Nat.*

- 1415 Decandia, F. A., & Elter, P. (1972). La "zona" ofiolitifera del Bracco nel settore compreso fra Levanto e
1416 la Val Gravena (Apennino ligure). *Società Geologica Italiana Bulletin*, 11, 37-64.
- 1417 Decarlis, A., & Lualdi, A. (2008). Late Triassic-early Jurassic paleokarst from the Ligurian Alps and its
1418 geological significance (Siderolitico Auct., Ligurian Briançonnais domain). *Swiss Journal of*
1419 *Geosciences*, 101(3), 579-593.
- 1420 Decarlis, A., Manatschal, G., Hauptert, I., & Masini, E. (2015). The tectono-stratigraphic evolution of
1421 distal, hyper-extended magma-poor conjugate rifted margins: Examples from the Alpine Tethys
1422 and Newfoundland–Iberia. *Marine and Petroleum Geology*, 68, 54-72.
- 1423 Decarlis, A., Beltrando, M., Manatschal, G., Ferrando, S., Carosi, R., 2017. Architecture of the Distal
1424 Piedmont-Ligurian Rifted Margin in NW Italy: Hints for a Flip of the Rift System Polarity.
1425 *Tectonics* 36, 2388–2406. <https://doi.org/10.1002/2017TC004561>
- 1426 Decarlis, A., Gillard, M., Tribuzio, R., Epin, M.E., Manatschal, G., 2018. Breaking up continents at
1427 magma-poor rifted margins: a seismic vs. outcrop perspective. *J. Geol. Soc. London*. jgs2018-
1428 041.
- 1429 De Graciansky, P. C., Roberts, D. G., & Tricart, P. (2011). The Western Alps, from rift to passive
1430 margin to orogenic belt: an integrated geoscience overview. Elsevier.
- 1431 Desmurs, L., Manatschal, G., & Bernoulli, D. (2001). The Steinmann Trinity revisited: mantle
1432 exhumation and magmatism along an ocean-continent transition: the Platta nappe, eastern
1433 Switzerland. *Geological Society, London, Special Publications*, 187(1), 235-266.
- 1434 Desmurs, L., Müntener, O., & Manatschal, G. (2002). Onset of magmatic accretion within a magma-
1435 poor rifted margin: a case study from the Platta ocean-continent transition, eastern Switzerland.
1436 *Contributions to Mineralogy and Petrology*, 144(3), 365-382.
- 1437 Dietrich, V. J. (1969). Die Ophiolithe des Oberhalbsteins (Graubünden) und das Ophiolithmaterial der
1438 ostschweizerischen Molasseablagerungen: ein petrographischer Vergleich (Doctoral dissertation,
1439 ETH Zurich).
- 1440 Dietrich, V., 1970. Die Stratigraphie der Platta-Decke: Fazielle Zusammenhänge zwischen
1441 Oberpenninikum und Unterostalpin. Geologisches Institut der Eidg. Technischen Hochschule
1442 und der Universität Zürich.
- 1443 Eberli G. P. (1985) Die jurassischen Sedimente in den ostalpinen Decken Graubündens. Dissertation.
1444 ETH Zurich, Zurich
- 1445 Eberli, G. P. (1987). Carbonate turbidite sequences deposited in rift-basins of the Jurassic Tethys
1446 Ocean (eastern Alps, Switzerland). *Sedimentology*, 34(3), 363-388.
- 1447 Eberli, G.P., 1988. The evolution of the southern continental margin of the Jurassic Tethys Ocen as
1448 recorded in the Allgäu Formation of the Austroalpine Nappes of Graubünden (Switzerland).
1449 *Eclogae Geol. Helv.* 81, 175--214.

- 1450 Epin, M.-E., Manatschal, G., Amann, M., Ribes, C., Clause, A., Guffon, T., Lescanne, M., 2019.
1451 Polyphase tectono-magmatic evolution during mantle exhumation in an ultra-distal, magma-poor
1452 rift domain: example of the fossil Platta ophiolite, SE Switzerland. *Int. J. Earth Sci.*
1453 <https://doi.org/10.1007/s00531-019-01772-0>
- 1454 Epin, M.E., Manatschal, G., 2018. Three-dimensional architecture, structural evolution, and role of
1455 inheritance controlling detachment faulting at a hyperextended distal margin: the example of the
1456 Err detachment system (SE Switzerland). *Tectonics* 37, 4494–4514.
1457 <https://doi.org/10.1029/2018TC005125>
- 1458 Epin, M.E., Manatschal, G., Amann, M., 2017. Defining diagnostic criteria to describe the role of rift
1459 inheritance in collisional orogens: the case of the Err-Platta nappes (Switzerland). *Swiss J.*
1460 *Geosci.* 110, 419–438. <https://doi.org/10.1007/s00015-017-0271-6>
- 1461 Escher, A., Masson, H., & Steck, A. (1993). Nappe geometry in the western Swiss Alps. *Journal of*
1462 *structural Geology*, 15(3-5), 501-509.
- 1463 Ferrando, S., Bernoulli, D., & Compagnoni, R. (2004). The Canavese zone (internal Western Alps): a
1464 distal margin of Adria. *Schweizerische Mineralogische und Petrographische Mitteilungen*, 84(1-
1465 20).
- 1466 Finger, W. (1978). Die zone von Samaden (unterostalpine Decken, Graubünden) und ihre
1467 jurassischen Brekzien (Doctoral dissertation, ETH Zurich).
- 1468 Flament, N; Gurnis, M., and Muller, R.D, (2013). A review of observations and models of dynamic
1469 topography. *Lithosphere* 2013;; 5 (2): 189–210. doi: <https://doi.org/10.1130/L245.1>
- 1470 Florineth, D., Froitzheim, N., 1994. Transition from continental to oceanic basement in the Tasna
1471 Nappe: evidence for Early Cretaceous opening of the Valais Ocean. *Schweiz. Miner. Petrogr.*
1472 *Mitt.* 74, 437–448.
- 1473 Frisch, W., 1979. Tectonic progradation and plate tectonic evolution of the Alps. *Tectonophysics* 60,
1474 121–139. [https://doi.org/10.1016/0040-1951\(79\)90155-0](https://doi.org/10.1016/0040-1951(79)90155-0)
- 1475 Frizon de Lamotte, D., Fourdan, B., Leleu, S., Leparmentier, F., Clarens, P., 2015. Style of rifting and
1476 the stages of Pangea breakup. *Tectonics* 34, 1–21.
1477 <https://doi.org/10.1002/2014TC003760>.Received
- 1478 Froitzheim, N. (1988). Synsedimentary and synorogenic normal faults within a thrust sheet of the
1479 Eastern Alps (Ortler zone, Graubünden, Switzerland). *Eclogae Geologicae Helveticae*, 81(3), 593-
1480 610.
- 1481 Froitzheim, N., Eberli, G.P., 1990. Extensional detachment faulting in the evolution of a Tethys passive
1482 continental margin, Eastern Alps, Switzerland. *Geol. Soc. Am. Bull.* 102, 1297–1308.
1483 [https://doi.org/10.1130/0016-7606\(1990\)102](https://doi.org/10.1130/0016-7606(1990)102)
- 1484 Froitzheim, N., Manatschal, G., 1996. Kinematics of Jurassic rifting, mantle exhumation, and passive-

- 1485 margin formation in the Austroalpine and Penninic nappes (eastern Switzerland). *Bull. Geol. Soc.*
1486 *Am.* 108, 1120–1133. [https://doi.org/10.1130/0016-7606\(1996\)108<1120:KOJRME>2.3.CO;2](https://doi.org/10.1130/0016-7606(1996)108<1120:KOJRME>2.3.CO;2)
- 1487 Furrer H (1985) Field Workshop on Triassic and Jurassic Sediments in the Eastern Alps of
1488 Switzerland: 25th.-29th. August 1985: Guide Book. Geologisches Institut ETH-Zürich, Zurich
- 1489 Gawthorpe, R.L., Leeder, M.R., 2000. Tectono-sedimentary evolution of active extensional basins.
1490 *Basin Res.* 12, 195–218. <https://doi.org/10.1111/j.1365-2117.2000.00121.x>Gupta, S., Cowie, P.
1491 A., Dawers, N. H., Underhill, J. R. (1998); A mechanism to explain rift-basin subsidence and
1492 stratigraphic patterns through fault-array evolution. *Geology* 26 (7): 595–598. doi:
1493 [https://doi.org/10.1130/0091-7613\(1998\)026<0595:AMTERB>2.3.CO;2](https://doi.org/10.1130/0091-7613(1998)026<0595:AMTERB>2.3.CO;2)Handy, M.R., M. Schmid,
1494 S., Bousquet, R., Kissling, E., Bernoulli, D., 2010. Reconciling plate-tectonic reconstructions of
1495 Alpine Tethys with the geological-geophysical record of spreading and subduction in the Alps.
1496 *Earth-Science Rev.* 102, 121–158. <https://doi.org/10.1016/j.earscirev.2010.06.002>
- 1497 Haug, E. (1892). Sur la continuation vers le sud des plis de la Dent du Midi. *Bull. Soc. géol. Fr.*, (3),
1498 20, p. CLXXXIV-CLXXXIX, séance du 19 décembre 1892, avec remarque de M. Bertrand.
- 1499 Haug, E., 1909. Les géosynclinaux de la chaîne des Alpes pendant les temps secondaires. Gauthier-
1500 Villars.
- 1501 Hauptert, I., Manatschal, G., Decarlis, A., Unternehr, P., 2016. Upper-plate magma-poor rifted margins:
1502 stratigraphic architecture and structural evolution. *Mar. Pet. Geol.* 69, 241–261.
1503 <https://doi.org/10.1016/j.marpetgeo.2015.10.020>
- 1504 Hendry, H. E. (1972). Breccias deposited by mass flow in the Breccia Nappe of the French pre-Alps.
1505 *Sedimentology*, 18(3-4), 277-292.
- 1506 Hermann, J., Müntener, O., Trommsdorff, V., Hansmann, W., Piccardo, G.B., 1997. Fossil crust-to-
1507 mantle transition, Val Malenco (Italian Alps). *J. Geophys. Res.* 102, 20123.
1508 <https://doi.org/10.1029/97JB01510>
- 1509 Hsü, K.J., Briegel, U., 1991. *Geologie der Schweiz. Switzerland.*
- 1510 Incerpi, N., Martire, L., Manatschal, G., Bernasconi, S.M., 2017. Evidence of hydrothermal fluid flow in
1511 a hyperextended rifted margin: the case study of the Err nappe (SE Switzerland). *Swiss J.*
1512 *Geosci.* 110, 439–456. <https://doi.org/10.1007/s00015-016-0235-2>
- 1513 Incerpi, N., Martire, L., Manatschal, G., Bernasconi, S.M., Gerdes, A., Czuppon, G., Palcsu, L.,
1514 Karner, G.D., Johnson, C.A., Figueredo, P.H., 2020. Hydrothermal fluid flow associated to the
1515 extensional evolution of the Adriatic rifted margin: Insights from the pre- to post-rift sedimentary
1516 sequence (SE Switzerland, N Italy). *Basin Res.* 32, 91–115. <https://doi.org/10.1111/bre.12370>
- 1517 Jagoutz, O., Müntener, O., Manatschal, G., Rubatto, D., Péron-Pinvidic, G., Turrin, B.D., Villa, I.M.,
1518 2007. The rift-to-drift transition in the North Atlantic: A stuttering start of the MORB machine?
1519 *Geology* 35, 1087–1090. <https://doi.org/10.1130/G23613A.1>

- 1520 Kaczmarek, M.-A., Müntener, O., 2008. Juxtaposition of Melt Impregnation and High-Temperature
1521 Shear Zones in the Upper Mantle; Field and Petrological Constraints from the Lanzo Peridotite
1522 (Northern Italy). *J. Petrol.* 49, 2187–2220. <https://doi.org/10.1093/petrology/egn065>
- 1523 Kilian, W., 1891. Sur quelques Céphalopodes nouveaux ou peu connus de la période secondaire.
- 1524 Lagabrielle, Y., & Cannat, M. (1990). Alpine Jurassic ophiolites resemble the modern central Atlantic
1525 basement. *Geology*, 18(4), 319-322.
- 1526 Lagabrielle, Y., 1994. Ophiolites of the southwestern Alps and the structure of the Tethyan oceanic
1527 lithosphere. *Ofioliti* 19, 413–434.
- 1528 Lagabrielle, Y., Vitale Brovarone, A., Ildefonse, B., 2015. Fossil oceanic core complexes recognized in
1529 the blueschist metaophiolites of Western Alps and Corsica. *Earth-Science Rev.*
1530 <https://doi.org/10.1016/j.earscirev.2014.11.004>
- 1531 Landry, P. (1978): Données nouvelles sur la couverture sédimentaire des massifs cristallins externes
1532 au Sud du Mont-Blanc. -*Géol. alp. (Grenoble)* 54, 83-112.
- 1533 Lavier, L.L., Manatschal, G., 2006. A mechanism to thin the continental lithosphere at magma-poor
1534 margins. *Nature* 440, 324–328. <https://doi.org/10.1038/nature04608>
- 1535 Le Breton, E., Brune, S., Ustaszewski, K., Zahirovic, S., Seton, M., & Müller, R. D. (2020). Kinematics
1536 and extent of the Piemonte-Liguria Basin—implications for subduction processes in the Alps. *Solid*
1537 *Earth Discussions*, 1-42.
- 1538 Lemoine, M., 1961. La marge externe de la fosse piémontaise dans les Alpes occidentales. *Rev.*
1539 *Géogr. phys. Géol. dyn* 2, 163–180.
- 1540 Lemoine, M. (1967). Brèches sédimentaires marines à la frontière entre les domaines Briançonnais et
1541 piémontais dans les Alpes occidentales. *Geologische Rundschau*, 56(1), 320-335.
- 1542 Lemoine, M., Bas, T., Arnaud-Vanneau, A., Arnaud, H., Dumont, T., Gidon, M., Bourbon, M., de
1543 Graciansky, P.C., Rudkiewicz, J.L., Megard-Galli, J., Tricart, P., 1986. The continental margin of
1544 the Mesozoic Tethys in the Western Alps. *Mar. Pet. Geol.* 3, 179–199.
1545 [https://doi.org/10.1016/0264-8172\(86\)90044-9](https://doi.org/10.1016/0264-8172(86)90044-9)
- 1546 Lemoine, M., Tricart, P., Boillot, G., 1987. Ultramafic and gabbroic ocean floor of the Ligurian Tethys
1547 (Alps, Corsica, Apennines): In search of a genetic model. *Geology* 15, 622–625.
1548 [https://doi.org/10.1130/0091-7613\(1987\)15](https://doi.org/10.1130/0091-7613(1987)15)
- 1549 Lescoutre, R., Manatschal, G., 2020. Role of rift-inheritance and segmentation for orogenic evolution:
1550 example from the Pyrenean-Cantabrian system. *Tectonics*.
- 1551 Li, X.-H.H., Faure, M., Lin, W., Manatschal, G., 2013. New isotopic constraints on age and magma
1552 genesis of an embryonic oceanic crust: The Chenaillet Ophiolite in the Western Alps. *Lithos* 160–

- 1553 161, 283–291. <https://doi.org/10.1016/j.lithos.2012.12.016>
- 1554 Lory, C., 1866. Sur le gisement de la Terebratula diphya dans les calcaires de la Porte-de-France, aux
1555 environs de Grenoble et de Chambéry. Bull. la Soc. Geol. Fr. 2, 516–521.
- 1556 Lory, C., 1860. Description géologique du Dauphiné pour servir d'explication à la carte géologique de
1557 cette province.
- 1558 MacLeod, C. J., Searle, R. C., Murton, B. J., Casey, J. F., Mallows, C., Unsworth, S. C., ... & Harris, M.
1559 (2009). Life cycle of oceanic core complexes. Earth and Planetary Science Letters, 287(3-4),
1560 333-344.
- 1561 Manatschal, G. (1999). Fluid-and reaction-assisted low-angle normal faulting: evidence from rift-
1562 related brittle fault rocks in the Alps (Err Nappe, eastern Switzerland). Journal of Structural
1563 Geology, 21(7), 777-793.
- 1564 Manatschal, G., Engström, A., Desmurs, L., Schaltegger, U., Cosca, M., Müntener, O., Bernoulli, D.,
1565 2006. What is the tectono-metamorphic evolution of continental break-up: The example of the
1566 Tasna Ocean-Continent Transition. J. Struct. Geol. 28, 1849–1869.
1567 <https://doi.org/10.1016/j.jsg.2006.07.014>
- 1568 Manatschal, G., Müntener, O., 2009. A type sequence across an ancient magma-poor ocean--
1569 continent transition: the example of the western Alpine Tethys ophiolites. Tectonophysics 473, 4–
1570 19. <https://doi.org/10.1016/j.tecto.2008.07.021>
- 1571 Manatschal, G., Nievergelt, P., 1997. A continent-ocean transition recorded in the Err and Platta
1572 nappes (Eastern Switzerland). Eclogae Geol. Helv. 90, 3–27.
- 1573 Manatschal, G., Sauter, D., Karpoff, A.M., Masini, E., Mohn, G., Lagabrielle, Y., 2011. The Chenaillet
1574 Ophiolite in the French/Italian Alps: An ancient analogue for an Oceanic Core Complex? Lithos
1575 124, 169–184. <https://doi.org/10.1016/j.lithos.2010.10.017>
- 1576 Manatschal, G., Chenin, P., Lescoutre, R., Miró, J., Cadenas, P., Saspiturry, N., Masini, E., Chevrot,
1577 S., Ford, M., Jolivet, L., Mouthereau, F., Thion, I., Issautier, B., and Calassou, S. (2021). The
1578 role of inheritance in forming rifts and rifted margins and building collisional orogens: a Biscay-
1579 Pyrenean perspective; BSGF, DOI: <https://doi.org/10.1051/bsgf/2021042> Marroni, M., Feroni,
1580 A.C., Di Biase, D., Ottria, G., Pandolfi, L., Taini, A., 2002. Polyphase folding at upper structural
1581 levels in the Borbera Valley (northern Apennines, Italy): Implications for the tectonic evolution of
1582 the linkage area between Alps and Apennines. Comptes Rendus - Geosci. 334, 565–572.
1583 [https://doi.org/10.1016/S1631-0713\(02\)01784-4](https://doi.org/10.1016/S1631-0713(02)01784-4)
- 1584 Masini, E., Manatschal, G., Mohn, G., Ghienne, J. F., & Lafont, F. (2011). The tectono-sedimentary
1585 evolution of a supra-detachment rift basin at a deep-water magma-poor rifted margin: The example of
1586 the Samedan Basin preserved in the Err nappe in SE Switzerland. *Basin Research*, 23(6), 652-677.
- 1587 Masini, E., Manatschal, G., Mohn, G., 2013. The Alpine Tethys rifted margins: Reconciling old and
1588 new ideas to understand the stratigraphic architecture of magma-poor rifted margins.
1589 *Sedimentology* 60, 174–196. <https://doi.org/10.1111/sed.12017>

- 1590 Masini, E., Manatschal, G., Mohn, G., Unternehr, P., 2012. Anatomy and tectono-sedimentary
1591 evolution of a rift-related detachment system: The example of the Err detachment (central Alps,
1592 SE Switzerland). *Bull. Geol. Soc. Am.* 124, 1535–1551. <https://doi.org/10.1130/B30557.1>
- 1593 McCarthy, A., Müntener, O., 2015. Ancient depletion and mantle heterogeneity: Revisiting the
1594 Permian-Jurassic paradox of Alpine peridotites. *Geology* 43, 255–258.
1595 <https://doi.org/10.1130/G36340.1>
- 1596 McCarthy, A., Tugend, J., Mohn, G., Candioti, L., Chelle-Michou, C., Arculus, R., Schmalholz, S.M.,
1597 Müntener, O., 2020. A case of Ampferer-type subduction and consequences for the Alps and the
1598 Pyrenees. *Am. J. Sci.* 320, 313–372. <https://doi.org/10.2475/04.2020.01>
- 1599 McKenzie, D. (1978). Some remarks on the development of sedimentary basins. *Earth and Planetary*
1600 *science letters*, 40(1), 25-32.
- 1601 Mohn, G., Manatschal, G., Beltrando, M., Hauptert, I., 2014. The role of rift-inherited hyper-extension in
1602 Alpine-type orogens. *Terra Nov.* 26, 347–353. <https://doi.org/10.1111/ter.12104>
- 1603 Mohn, G., Manatschal, G., Beltrando, M., Masini, E., Kuzsnir, N., 2012. Necking of continental crust in
1604 magma-poor rifted margins: Evidence from the fossil Alpine Tethys margins. *Tectonics* 31,
1605 TC1012. <https://doi.org/10.1029/2011TC002961>
- 1606 Mohn, G., Manatschal, G., Masini, E., Müntener, O., 2011. Rift-related inheritance in orogens: a case
1607 study from the Austroalpine nappes in Central Alps (SE-Switzerland and N-Italy). *Int. J. Earth*
1608 *Sci.* 100, 937–961. <https://doi.org/10.1007/s00531-010-0630-2>
- 1609 Mohn, G., Manatschal, G., Müntener, O., Beltrando, M., Masini, E., 2010. Unravelling the interaction
1610 between tectonic and sedimentary processes during lithospheric thinning in the Alpine Tethys
1611 margins. *Int. J. Earth Sci.* 99, 75–101. <https://doi.org/10.1007/s00531-010-0566-6>
- 1612 Montadert, L., de Charpal, O., Roberts, D., Guennoc, P., Sibuet, J.-C., 1979. Northeast Atlantic
1613 passive continental margins: Rifting and subsidence processes, in: Talwani, M., Hay, W., Ryan,
1614 W.B.F. (Eds.), *Deep Drilling Results in the Atlantic Ocean: Continental Margins and*
1615 *Paleoenvironment*, Volume 3. American Geophysical Union (AGU), pp. 154–186.
1616 <https://doi.org/10.1029/me003p0154>
- 1617 Müntener, O., Manatschal, G., Desmurs, L., Pettke, T., 2010. Plagioclase peridotites in ocean-
1618 continent transitions: Refertilized mantle domains generated by melt stagnation in the shallow
1619 mantle lithosphere. *J. Petrol.* 51, 255–294. <https://doi.org/10.1093/petrology/egp087>
- 1620 Müntener, O., Pettke, T., Desmurs, L., Meier, M., Schaltegger, U., 2004. Refertilization of mantle
1621 peridotite in embryonic ocean basins: trace element and Nd isotopic evidence and implications
1622 for crust-mantle relationships. *Earth Planet. Sci. Lett.* 221, 293–308.
1623 [https://doi.org/10.1016/S0012-821X\(04\)00073-1](https://doi.org/10.1016/S0012-821X(04)00073-1)
- 1624 Müntener, O., Piccardo, G.B., 2003. Melt migration in ophiolitic peridotites: the message from Alpine-
1625 Apennine peridotites and implications for embryonic ocean basins. *Geol. Soc. London, Spec.*
1626 *Publ.* 218, 69–89. <https://doi.org/10.1144/GSL.SP.2003.218.01.05>

- 1627 Nirrengarten, M., Manatschal, G., Tugend, J., Kuszniir, N., Sauter, D., 2018. Kinematic Evolution of the
1628 Southern North Atlantic: Implications for the Formation of Hyperextended Rift Systems.
1629 *Tectonics* 37, 89–118. <https://doi.org/10.1002/2017TC004495>
- 1630 Nirrengarten, M., Manatschal, G., Tugend, J., Kuszniir, N.J., Sauter, D., 2017. Nature and origin of the
1631 J-magnetic anomaly offshore Iberia – Newfoundland: implications for plate reconstructions. *Terra*
1632 *Nov.* 29, 20–28. <https://doi.org/10.1111/ter.12240>
- 1633 Nirrengarten, M., Manatschal, G., Yuan, X. P., Kuszniir, N. J., & Maillot, B. (2016). Application of the
1634 critical Coulomb wedge theory to hyper-extended, magma-poor rifted margins. *Earth and*
1635 *Planetary Science Letters*, 442, 121-132.
- 1636 Péron-Pinvidic, G., & Manatschal, G. (2019). Rifted margins: state of the art and future challenges.
1637 *Frontiers in Earth Science*, 7, 218. Petri, B., Duretz, T., Mohn, G., Schmalholz, S.M., Karner,
1638 G.D., Müntener, O., 2019. Thinning mechanisms of heterogeneous continental lithosphere. *Earth*
1639 *Planet. Sci. Lett.* 512, 147–162. <https://doi.org/10.1016/J.EPSL.2019.02.007>
- 1640 Petri, B., Mohn, G., Štípská, P., Schulmann, K., Manatschal, G., 2016. The Sondalo gabbro contact
1641 aureole (Campo unit, Eastern Alps): implications for mid-crustal mafic magma emplacement.
1642 *Contrib. to Mineral. Petrol.* 171, 52. <https://doi.org/10.1007/s00410-016-1263-7>
- 1643 Petri, B., Skrzypek, E., Mohn, G., Mateeva, T., Galster, F., Manatschal, G., 2017. U–Pb
1644 geochronology of the Sondalo gabbroic complex (Central Alps) and its position within the
1645 Permian post-Variscan extension. *Int. J. Earth Sci.* <https://doi.org/10.1007/s00531-017-1465-x>
- 1646 Picazo, S., Müntener, O., Manatschal, G., Bauville, A., Karner, G.D., Johnson, C., 2016. Mapping the
1647 nature of mantle domains in Western and Central Europe based on clinopyroxene and spinel
1648 chemistry: evidence for mantle modification during an extensional cycle. *Lithos.*
1649 <https://doi.org/10.1016/j.lithos.2016.08.02>
- 1650 Piccardo, G.B., Müntener, O., Zanetti, A., Romairone, A., Bruzzone, S., Poggi, E., Spagnolo, G., 2004.
1651 The Lanzo South peridotite: melt/peridotite interaction in the mantle lithosphere of the Jurassic
1652 Ligurian Tethys. *Ophioliti* 29, 37–62. <https://doi.org/10.4454/OFIOLITI.V29I1.205>
- 1653 Piccardo, G.B., Rampone, E., Vannucci, R., 1990. Upper mantle evolution during continental rifting
1654 and ocean formation: evidences from peridotite bodies of the western Alpine-northern Apennine
1655 system. *Mémoires la Société géologique Fr.* 156, 323–333.
- 1656 Piccardo, G.B., Zanetti, A., Müntener, O., 2007. Melt/peridotite interaction in the Southern Lanzo
1657 peridotite: Field, textural and geochemical evidence. *Lithos* 94, 181–209.
1658 <https://doi.org/10.1016/j.lithos.2006.07.002>
- 1659 Pinto, V.H.G., Manatschal, G., Karpoff, A.-M., Viana, A., 2015. Tracing mantle-reacted fluids in
1660 magma-poor rifted margins: The example of Alpine Tethyan rifted margins. *Geochemistry,*
1661 *Geophys. Geosystems* 16, 3271–3308. <https://doi.org/10.1002/2015GC005830>
- 1662 Pinto, V. H. G., Manatschal, G., Karpoff, A. M., Ulrich, M., & Viana, A. R. (2017). Seawater storage
1663 and element transfer associated with mantle serpentinization in magma-poor rifted margins: A

- 1664 quantitative approach. *Earth and Planetary Science Letters*, 459, 227-237. Quick, J.E., Sinigoi,
1665 S., Negri, L., Demarchi, G., Mayer, A., 1992. Synmagmatic deformation in the underplated
1666 igneous complex of the Ivrea-Verbanò zone. *Geology* 20, 613–616. [https://doi.org/10.1130/0091-7613\(1992\)020<0613:sditui>2.3.co;2](https://doi.org/10.1130/0091-7613(1992)020<0613:sditui>2.3.co;2)
1667
- 1668 Rampone, E., Borghini, G., Basch, V., 2020. Melt migration and melt-rock reaction in the Alpine-
1669 Apennine peridotites: Insights on mantle dynamics in extending lithosphere. *Geosci. Front.* 11,
1670 151–166. <https://doi.org/10.1016/j.gsf.2018.11.001>
- 1671 Rampone, E., Hofmann, A.W., Piccardo, G.B., Vannucci, R., Bottazzi, P., Ottolini, L., 1995. Petrology,
1672 mineral and isotope geochemistry of the external Liguride peridotites (Northern Apennines, Italy).
1673 *J. Petrol.* 36, 81–105. <https://doi.org/10.1093/petrology/36.1.81>
- 1674 Rampone, E., Hofmann, A.W., Raczek, I., 1998. Isotopic contrasts within the Internal Liguride ophiolite
1675 (N. Italy): the lack of a genetic mantle–crust link. *Earth Planet. Sci. Lett.* 163, 175–189.
1676 [https://doi.org/10.1016/S0012-821X\(98\)00185-X](https://doi.org/10.1016/S0012-821X(98)00185-X)
- 1677 Rampone, E., Piccardo, G.B., Vannucci, R., Bottazzi, P., 1997. Chemistry and origin of trapped melts
1678 in ophiolitic peridotites. *Geochim. Cosmochim. Acta* 61, 4557–4569.
1679 [https://doi.org/10.1016/s0016-7037\(97\)00260-3](https://doi.org/10.1016/s0016-7037(97)00260-3)
- 1680 Renna, M.R., Tribuzio, R., Sanfilippo, A., Thirlwall, M., 2018. Role of melting process and melt–rock
1681 reaction in the formation of Jurassic MORB-type basalts (Alpine ophiolites). *Contrib. to Mineral.
1682 Petrol.* 173, 1–21. <https://doi.org/10.1007/s00410-018-1456-3>
- 1683 Ribes, C., Ghienne, J.F., Manatschal, G., Dall’Asta, N., Stockli, D.F., Galster, F., Gillard, M., Karner,
1684 G.D., 2020a. The Grès Singuliers of the Mont Blanc region (France and Switzerland):
1685 stratigraphic response to rifting and crustal necking in the Alpine Tethys. *Int. J. Earth Sci.* 109,
1686 2325–2352. <https://doi.org/10.1007/s00531-020-01902-z>
- 1687 Ribes, C., Ghienne, J. F., Manatschal, G., Decarlis, A., Karner, G. D., Figueredo, P. H., & Johnson, C.
1688 A. (2019b). Long-lived mega fault-scarps and related breccias at distal rifted margins: insights
1689 from present-day and fossil analogues. *Journal of the Geological Society*, 176(5), 801-816.
- 1690 Ribes, C., Manatschal, G., Ghienne, J.-F., Karner, G.D., Johnson, C.A., Figueredo, P.H., Incerpi, N.N.,
1691 Epin, M., 2019a. The syn-rift stratigraphic record across a fossil hyper-extended rifted margin:
1692 the example of the northwestern Adriatic margin exposed in the Central Alps. *Int. J. Earth Sci.*
1693 108, 2071–2095. <https://doi.org/DOI: 10.1007/s00531-019-01750-6>
- 1694 Ribes, C., Petri, B., Ghienne, J., Manatschal, G., Galster, F., Karner, G.D., Figueredo, P.H., Johnson,
1695 C.A., Karpoff, A., 2020b. Tectono-sedimentary evolution of a fossil ocean-continent transition:
1696 Tasna nappe, central Alps (SE Switzerland). *Geol. Soc. Am. Bull.* 1–20.
1697 <https://doi.org/10.1130/B35310.1/4863878/b35310.pdf>
- 1698 Robertson, A. H. F., & Searle, M. P. (1990). The northern Oman Tethyan continental margin:
1699 stratigraphy, structure, concepts and controversies. Geological Society, London, Special
1700 Publications, 49(1), 3-25.
- 1701 Rosenbaum, G., Lister, G.S., Duboz, C., 2002. Relative motions of Africa, Iberia and Europe during

- 1702 Alpine orogeny. *Tectonophysics* 359, 117–129. [https://doi.org/10.1016/S0040-1951\(02\)00442-0](https://doi.org/10.1016/S0040-1951(02)00442-0)
- 1703 Sanfilippo, A., Salters, V., Tribuzio, R., Zanetti, A., 2019. Role of ancient, ultra-depleted mantle in Mid-
1704 Ocean-Ridge magmatism. *Earth Planet. Sci. Lett.* 511, 89–98.
1705 <https://doi.org/10.1016/j.epsl.2019.01.018>
- 1706 Sauter, D., Cannat, M., Rouméjon, S., Andreani, M., Birot, D., Bronner, A., Brunelli, D., Carlut, J.,
1707 Delacour, A., Guyader, V., MacLeod, C.J., Manatschal, G., Mendel, V., Ménez, B., Pasini, V.,
1708 Ruellan, E., Searle, R., 2013. Continuous exhumation of mantle-derived rocks at the Southwest
1709 Indian Ridge for 11 million years. *Nat. Geosci.* 6, 314–320. <https://doi.org/10.1038/ngeo1771>
- 1710 Schaltegger, U., Desmurs, L., Manatschal, G., Müntener, O., Meier, M., Frank, M., & Bernoulli, D.
1711 (2002). The transition from rifting to sea-floor spreading within a magma-poor rifted margin: Field
1712 and isotopic constraints. *Terra Nova*, 14(3), 156-162.
- 1713 Schettino, A., & Turco, E. (2011). Tectonic history of the western Tethys since the Late Triassic.
1714 *Bulletin*, 123(1-2), 89-105. Schmid, S.M., Fgenschuh, B., Kissling, E., Schuster, R., Fügenschuh,
1715 B., 2004. Tectonic map and overall architecture of the Alpine orogen. *Eclogae Geol. Helv.* 97,
1716 93–117. <https://doi.org/10.1007/s00015-004-1113-x>
- 1717 Schmid, S.M., Pfiffner, O.A., Froitzheim, N., Schönborn, G., Kissling, E., 1996. Geophysical-geological
1718 transect and tectonic evolution of the Swiss-Italian Alps. *Tectonics* 15, 1036–1064.
1719 <https://doi.org/10.1029/96TC00433>
- 1720 Şengör, A.M.C., 2014. Eduard Suess and Global Tectonics: an Illustrated 'Short Guide'. *Austrian J.*
1721 *Earth Sci.* 107, 6–82.
- 1722 Speranza, F., Minelli, L., Pignatelli, A., Chiappini, M., 2012. The Ionian Sea: The oldest in situ ocean
1723 fragment of the world? *J. Geophys. Res. B Solid Earth* 117.
1724 <https://doi.org/10.1029/2012JB009475>
- 1725 Stampfli, G. M., 1993, Le Briançonnais, terrain exotique dans les Alpes?: *Eclogae Geologicae*
1726 *Helvetiae*, v. 86,p. 1–45.
- 1727 Stampfli, G. M. (2000). Tethyan oceans. *Geological society, london, special*
1728 *publications*, 173(1), 1-23. Steffen, D., Jaques, C., Nydegger, T. H., Petroons, D., & Wildi,
1729 W. (1993). La Brèche du Chablais à son extrémité occidentale (Hte Savoie, France):
1730 Sédimentologie, éléments stratigraphiques et interprétation paléogéographique. *Eclogae*
1731 *Geologicae Helvetiae*, 86(2), 543-568.
- 1732 Steinmann, G., 1905. *Geologische Beobachtungen in den Alpen*. Wagners Universitäts-
1733 Buchdruckerei.
- 1734 Suess, E., 1875. *Die Entstehung der Alpen*. Braumüller. Wien.
- 1735 Suess, E., 1883. *Das Antlitz der Erde, Ia (Erste Abtheilung)*. F. Tempsky, Prag G. Freytag, Leipzig
1736 310.

- 1737 Sutra, E., Manatschal, G., Mohn, G., & Unternehr, P. (2013). Quantification and restoration of
1738 extensional deformation along the Western Iberia and Newfoundland rifted margins.
1739 *Geochemistry, Geophysics, Geosystems*, 14(8), 2575-2597.
- 1740 Szameitat, L. S., Manatschal, G., Nirrengarten, M., Ferreira, F. J., & Heilbron, M. (2020). Magnetic
1741 characterization of the zigzag shaped J-anomaly: Implications for kinematics and breakup
1742 processes at the Iberia–Newfoundland margins. *Terra Nova*, 32(5), 369-380.
- 1743 Tavani, S., Bertok, C., Granado, P., Piana, F., Salas, R., Vigna, B., Muñoz, J.A., 2018. The Iberia-
1744 Eurasia plate boundary east of the Pyrenees. *Earth-Science Rev.*
1745 <https://doi.org/10.1016/j.earscirev.2018.10.008>
- 1746 Termier, P. (1899). Les nappes de recouvrement du Briançonnais. *Bull. Soc. géol. France*, (3),27, p.
1747 47-84
- 1748 Tribuzio, R., Thirlwall, M.F., Vannucci, R., 2004. Origin of the Gabbro–Peridotite Association from the
1749 Northern Apennine Ophiolites (Italy). *J. Petrol.* 45, 1109–1124.
1750 <https://doi.org/10.1093/petrology/egh006>
- 1751 Tricart, P., & Lemoine, M. (1988). A l'origine de la structure des Schistes lustrés à ophiolites du
1752 Queyras (Alpes françaises): un mode atypique d'obduction, conséquence de la structure
1753 particulière de la croûte océanique ligure. *Comptes rendus de l'Académie des sciences. Série 2,*
1754 *Mécanique, Physique, Chimie, Sciences de l'univers, Sciences de la Terre*, 306(4), 301-306.
- 1755 Trümpy, R. (1971) Stratigraphy in mountain belts. *Quart J Geol Soc Lond* 126:293–318
- 1756 Trümpy, R., 1975. Penninic-Austroalpine boundary in the Swiss Alps: a presumed former continental
1757 margins and its problems. *Am. J. Sci.* 275, 209–238.
- 1758 Trümpy, R. 1980: *Geology of Switzerland*. schweizerische Geologische Kom-mission, Wepf & co,
1759 basel.
- 1760 Tugend, J., Manatschal, G., Kuszniir, N.J., Masini, E., 2014. Characterizing and identifying structural
1761 domains at rifted continental margins: application to the Bay of Biscay margins and its Western
1762 Pyrenean fossil remnants. *Geol. Soc. London Spec. Publ.* 413, SP413--3.
1763 <https://doi.org/10.1002/2014TC003529>
- 1764 van Hinsbergen, D. J., Vissers, R. L., & Spakman, W. (2014). Origin and consequences of western
1765 Mediterranean subduction, rollback, and slab segmentation. *Tectonics*, 33(4), 393-419.
- 1766 Van Hinsbergen, D. J., Torsvik, T. H., Schmid, S. M., Mañenco, L. C., Maffione, M., Vissers, R. L., ... &
1767 Spakman, W. (2020). Orogenic architecture of the Mediterranean region and kinematic
1768 reconstruction of its tectonic evolution since the Triassic. *Gondwana Research*, 81, 79-229.
1769 Vissers, R.L.M., Meijer, P.T., 2012. Mesozoic rotation of Iberia: Subduction in the Pyrenees?
1770 *Earth-Science Rev.* 110, 93–110. <https://doi.org/10.1016/j.earscirev.2011.11.001>
- 1771 Weissert, H. J., & Bernoulli, D. (1985). A transform margin in the Mesozoic Tethys: evidence from the

- 1772 Swiss Alps. Geologische rundschau, 74(3), 665-679.
- 1773 Weidman, M. 1972. Le front de la Breche du Chablais dans le secteur de Saint-Jean-d'Aulph (Haute-
1774 Savoie). Géologie Alpine, 48, 229–246.
- 1775 Wernicke, B., 1985. Uniform-sense normal simple shear of the continental lithosphere. Can. J. Earth
1776 Sci. 22, 108–125. <https://doi.org/10.1139/e85-009>
- 1777 Whitmarsh, R.B., Manatschal, G., Minshull, T. a, 2001. Evolution of magma-poor continental margins
1778 from rifting to seafloor spreading. Nature 413, 150–154. <https://doi.org/10.1038/35093085>
- 1779 Wilson, R. C. L., Manatschal, G., & Wise, S. (2001). Rifting along non-volcanic passive margins:
1780 stratigraphic and seismic evidence from the Mesozoic successions of the Alps and western
1781 Iberia. Geological Society, London, Special Publications, 187(1), 429-452.
- 1782
- 1783 **Submitted**
- 1784 Chenin, P. Manatschal, G., Ghienne, J.-F., Chao, P. (this volume): The syn-rift tectono-stratigraphic
1785 evolution of rifted margins (Part II): a new model to break through the proximal/distal
1786 interpretation frontier
- 1787
- 1788